Contents

Chapter 8

Finite Element Method for Dynamics of Nonlocal Systems

This paper introduces the idea of nonlocal normal modes arising in the dynamic analysis of nanoscale structures. A nonlocal finite element approach is developed for the axial vibration of nanorods, bending vibration of nanobeams and transverse vibration of nanoplates. Explicit expressions of the element mass and stiffness matrices are derived in closed-form as functions of a length-scale parameter. In general the mass matrix can be expressed as a sum of the classical local mass matrix and a nonlocal part. The nonlocal part of the mass matrix is scale-dependent and vanishes for systems with larger length-scales. New analytical methods are developed to understand the dynamic behaviour of discrete nonlocal systems in the light of classical local systems. The conditions for the existence of classical normal modes for undamped and damped nonlocal systems are established. Closed-form approximate expressions of nonlocal natural frequencies, modes and frequency response functions are derived. Results derived in the paper are illustrated using examples of axial and bending vibration of nanotubes and transverse vibration of graphene sheets.

8.1. Introduction

Nanoscale systems, such as those fabricated from simple and complex nanorods, nanobeams [WON 97] and nanoplates have attracted keen interest among scientists and engineers. Examples of one-dimensional nanoscale objects include (nanorod and nanobeam) carbon nanotubes [IIJ 93], zinc oxide (ZnO) nanowires and boron nitride (BN) nanotubes, while two-dimensional nanoscale objects include graphene sheets [WAR 09] and BN nanosheets [PAC 08]. These nanoscale entities or nanostructures are found to have exciting mechanical, chemical, electrical, optical and electronic properties. Nanostructures are being used in the field of nanoelectronics, nanodevices, nanosensors, nano-oscillators, nano-actuators, nanobearings, and micromechanical resonators, transporter of drugs, hydrogen storage, electrical batteries, solar cells, nanocomposites and nanooptomechanical systems (NOMS). Understanding the dynamics of nanostructures is crucial for the development of future generation applications in these areas.

Experiments at the nanoscale can be difficult as many parameters need to be taken care of. On the other hand, atomistic computation methods such as molecular dynamic (MD) simulations [BRO 07] are computationally prohibitive for nanostructures with large numbers of atoms. Thus continuum mechanics is an important tool for modelling, understanding and predicting physical behaviour of nanostructures. Although continuum models based on classical elasticity are able to predict the general behaviour of nanostructures, they lack the accountability of effects arising from the small-scale. At small-scale the theory and laws of classical elasticity may not hold. Consequently for accurate predictions, the employability of the classical continuum models have been questioned in the analysis of nanostructures and nanoscale systems. To address this, size-dependent continuum based methods [AKG 11, AKG 12, JOM 11, KAH 10] are getting in popularity in the modelling of small sized structures as they offer much faster solutions than molecular dynamic simulations for various nano engineering problems.

Currently research efforts are undergoing to bring in the size-effects within the formulation by modifying the traditional classical mechanics. One popularly used size-dependant theory is the nonlocal elasticity theory pioneered by Eringen [ERI 83], and applied to nanotechnology by Peddieson et al [PED 03]. The theory of nonlocal elasticity (nonlocal continuum mechanics) is being increasingly used for efficient analysis of nanostructures viz. nanorods [AYD 09, AYD 12], nanobeams [MUR 12a], nanoplates [AKS 11, BAB 11], nanorings [WAN 08], carbon nanotubes [ART 11, AYD 11], graphenes [ANS 11, MUR 09], nanoswitches [YAN 08] and microtubules [HEI 10]. Nonlocal elasticity accounts for the small-scale effects at the atomistic level. At nanometer scales, size effects often become prominent. Both experimental and atomistic simulation results have shown a significant size-effect in the mechanical properties when the dimensions of these structures become small [KIA 98, TAN 08]. In the nonlocal elasticity theory the small-scale effects are captured by assuming that the stress at a point as a function of the strains at all points in the domain. Nonlocal theory considers long-range inter-atomic interaction and yields results dependent on the size of a body [ERI 83]. Some of the drawbacks of the classical continuum theory could be efficiently avoided and size-dependent phenomena can be explained by the nonlocal elasticity theory. A good review on nonlocal elasticity and application to nanostructures can be found in Ref [ARA 12].

Several researchers have used nonlocal theory for dynamic analysis of continuum systems such as nanorods, nanobeams and nanoplates. Nanorods have found application in energy harvesting, light emitting devices and microelectromechanical systems (MEMS). Using nonlocal elasticity, various work on mechanical behaviour of nanorods [AYD 09, AYD 12, MUR 11b, MUR 10, NAR 11a] were reported. Numerous works are seen in literature regarding analysis (mainly structural) of nanobeams using nonlocal elasticity [ARA 12] and coupled nanobeams [MUR 12a]. The work on nanobeams is related to carbon nanotubes, boron nitride nanotubes and ZnO nanowires. Nanoplate models have been used to represent two-dimensional nanostructures such as graphene sheets and BN sheets. Several works on dynamics of nanoplates using nonlocal theory are available in literature [PHA 10, MUR 11a].

From the brief literature review it is clear that significant research efforts have taken place in the analysis of nano structures modelled as a continuum. While the results have given significant insights, the analysis is normally restricted to single-structure (e.g, a beam or a plate) with simple boundary conditions and no damping. In the future complex nanoscale structures will be used for next generation nano electro mechanical systems. Therefore, it is necessary to have the ability for design and analysis of damped built-up structures. The finite element approach for nanoscale structures can provide this generality. Work on nonlocal finite elements is in its infancy stage. Pisano et al. [PIS 09] reported a finite element procedure for nonlocal integral elasticity. Chang [CHA 12] studied the small scale effects on axial vibration of non-uniform and nonhomogeneous nanorods by using the theory of nonlocal elasticity and the finite element method. Narendar and Gopalakrishnan [NAR 11b] used the concept of nonlocal elasticity and applied it for the development of a spectral finite element (SFE) for analysis of nanorods. Recently Adhikari et al. [ADH 13] reported the free and forced axial vibrations of damped nonlocal rods using dynamic nonlocal finite element analysis. Similar to the few works on nonlocal finite element analysis of nanorods, not many works were reported on the nonlocal finite element formulation of nanobeams (carbon nanotubes). Phadikar and Pradhan [PHA 10] have proposed basic finite element formulations for a nonlocal elastic Euler-Bernoulli beam using the Galerkin technique. Studies were carried out for bending, free vibration and buckling for nonlocal beam with four classical boundary conditions. Pradhan [PRA 12] updated the work of nonlocal finite element to Timoshenko beam theory and applied it to carbon nanotubes. With the finite element analysis bending, buckling and vibration for nonlocal beams with clamped-clamped, hinged-hinged, clamped-hinged and clamped-free boundary conditions were illustrated. The basic nonlocal finite elements of undamped two-dimensional nanoplates (such as graphene sheets) were reported by Phadikar and Pradhan [PHA 10]. Recently, Ansari et al [ANS 10] developed nonlocal finite element model for vibration of embedded multi-layered graphene sheets. The proposed finite elements were based on the Mindlin-type equations of motion coupled together through the van der Waals interaction. Vibrational characteristics of multi-layered graphene sheets with different boundary conditions embedded in an elastic medium were considered.

The majority of the reported works on nonlocal finite element analysis consider free vibration studies where the effect of non-locality on the undamped eigensolutions has been studied. Damped nonlocal systems and forced vibration response analysis have received little attention. On the other hand, significant body of literature is available [MEI 97, GÉR 97, PET 98] on finite element analysis of local dynamical systems. It is necessary to extend the ideas of local modal analysis to nonlocal systems to gain qualitative as well as quantitative understanding. This way, the dynamic behaviour of general nonlocal discretised systems can be explained in the light of well known established theories of discrete local systems. The purpose of this paper is make essential contributions in this open area.

The paper is organised as follows. In section 8.2 we introduce the nonlocal finite element formulation for the axial vibration of rods, bending vibration of beams and transverse vibration of plates. Explicit expressions of element mass and stiffness matrices for the three systems are derived. Modal analysis of discrete nonlocal dynamical systems is discussed in section 8.3. The conditions for the existence of classical normal modes, approximations for nonlocal frequencies and modes are proposed. In section 8.4 dynamics of damped nonlocal systems and approximation to the frequency response function are discussed. Analytical results, including the approximations of the nonlocal natural frequencies and modes, are numerically illustrated for the three systems in section 8.5. In section 8.6 some conclusions are drawn based on the theoretical and numerical results obtained in the paper.

8.2. Finite element modelling of nonlocal dynamic systems

8.2.1. *Axial vibration of nanorods*

The equation of motion of axial vibration for a damped nonlocal rod can be expressed as

$$\begin{aligned}EA\frac{\partial^2 U(x,t)}{\partial x^2}&+\widehat{c}_1\left(1-(e_0a)_1^2\frac{\partial^2}{\partial x^2}\right)\frac{\partial^3 U(x,t)}{\partial x^2\partial t}\\&=\widehat{c}_2\left(1-(e_0a)_2^2\frac{\partial^2}{\partial x^2}\right)\frac{\partial U(x,t)}{\partial t}+\left(1-(e_0a)^2\frac{\partial^2}{\partial x^2}\right)\left\{m\frac{\partial^2 U(x,t)}{\partial t^2}+F(x,t)\right\}\end{aligned}\quad(8.1)$$

In the above equation EA is the axial rigidity, m is mass per unit length, e_0a is the nonlocal parameter [ERI 83], $U(x,t)$ is the axial displacement, $F(x,t)$ is the applied force, x is the spatial variable and t is the time. The constant $\widehat{c}_1$ is the strain-rate-dependent viscous damping coefficient and $\widehat{c}_2$ is the velocity-dependent viscous damping coefficient. The parameters $(e_0a)_1$ and $(e_0a)_2$ are nonlocal parameters related to the two damping terms respectively. For simplicity the nonlocal effect in damping is ignored in this paper, that is, we consider $(e_0a)_1=(e_0a)_2=0$. We consider an element of length ℓ_e with axial stiffness EA and mass per unit length m. An element of the axially vibrating rod is shown in Figure 8.1. This element has two degrees of freedom and there are two shape functions

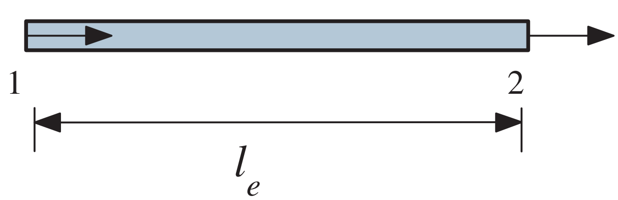

Figure 8.1 – A nonlocal element for the axially vibrating rod with two nodes. It has two degrees of freedom and the displacement field within the element is expressed by linear shape functions.

$N_1(x)$ and $N_2(x)$. The shape function matrix for the axial deformation [PET 98] can be given by

$$\mathbf{N}(x)=[N_1(x),N_2(x)]^T=[1-x/\ell_e,x/\ell_e]^T\quad(8.2)$$

Using this the stiffness matrix can be obtained using the conventional variational formulation as

$$\mathbf{K}_e = EA\int_0^{\ell_e} \frac{d\mathbf{N}(x)}{dx}\frac{d\mathbf{N}^T(x)}{dx}\mathrm{d}x = \frac{EA}{\ell_e}\begin{bmatrix} 1 & -1 \\ -1 & 1 \end{bmatrix} \tag{8.3}$$

The mass matrix for the nonlocal element can be obtained as

$$\begin{aligned}\mathbf{M}_e &= m\int_0^{\ell_e} \mathbf{N}(x)\mathbf{N}^T(x)\mathrm{d}x + m(e_0a)^2\int_0^{\ell_e} \frac{d\mathbf{N}(x)}{dx}\frac{d\mathbf{N}^T(x)}{dx}\mathrm{d}x \\ &= \frac{m\ell_e}{6}\begin{bmatrix} 2 & 1 \\ 1 & 2 \end{bmatrix} + \left(\frac{e_0a}{\ell_e}\right)^2 m\ell_e\begin{bmatrix} 1 & -1 \\ -1 & 1 \end{bmatrix}\end{aligned} \tag{8.4}$$

For the special case when the rod is local, the mass matrix derived above reduces to the classical mass matrix[PET 98, DAW 84] as $e_0a = 0$. Therefore for a nonlocal rod, the element stiffness matrix is identical to that of a classical local rod but the element mass has an additive term which is dependent on the nonlocal parameter.

8.2.2. *Bending vibration of nanobeams*

For the bending vibration of a nonlocal damped beam, the equation of motion can be expressed by

$$\begin{aligned}&EI\frac{\partial^4 V(x,t)}{\partial x^4} + m\left(1-(e_0a)^2\frac{\partial^2}{\partial x^2}\right)\left\{\frac{\partial^2 V(x,t)}{\partial t^2}\right\} \\ &+ \widehat{c}_1\left(1-(e_0a)_1^2\frac{\partial^2}{\partial x^2}\right)\frac{\partial^5 V(x,t)}{\partial x^4 \partial t} + \widehat{c}_2\left(1-(e_0a)_2^2\frac{\partial^2}{\partial x^2}\right)\frac{\partial V(x,t)}{\partial t} = \left(1-(e_0a)^2\frac{\partial^2}{\partial x^2}\right)\{F(x,t)\}\end{aligned} \tag{8.5}$$

In the above equation EI is the bending rigidity, m is mass per unit length, e_0a is the nonlocal parameter, $V(x,t)$ is the transverse displacement and $F(x,t)$ is the applied force. The constant $\widehat{c}_1$ is the strain-rate-dependent viscous damping coefficient and $\widehat{c}_2$ is the velocity-dependent viscous damping coefficient. The damping nonlocal parameters are assumed to be zero for simplicity. We consider an element of length ℓ_e with bending stiffness EI and mass per unit length m. An element of the beam is shown in Figure 8.2. This element has four degrees of freedom and

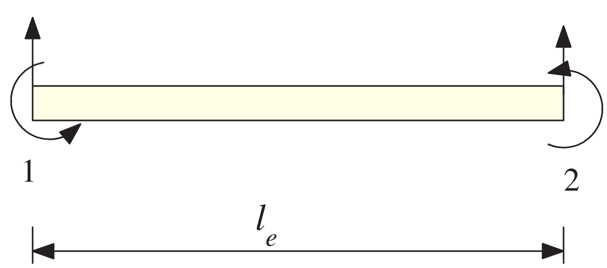

Figure 8.2 – A nonlocal element for the bending vibration of a beam. It has two nodes and four degrees of freedom. The displacement field within the element is expressed by cubic shape functions.

there are four shape functions. The shape function matrix for the bending deformation [PET 98] can be given by

$$\mathbf{N}(x) = [N_1(x), N_2(x), N_3(x), N_4(x)]^T \tag{8.6}$$

where

$$\begin{aligned}N_1(x) &= 1 - 3\frac{x^2}{\ell_e^2} + 2\frac{x^3}{\ell_e^3}, & N_2(x) &= x - 2\frac{x^2}{\ell_e} + \frac{x^3}{\ell_e^2}, \\ N_3(x) &= 3\frac{x^2}{\ell_e^2} - 2\frac{x^3}{\ell_e^3}, & N_4(x) &= -\frac{x^2}{\ell_e} + \frac{x^3}{\ell_e^2}\end{aligned} \tag{8.7}$$

Using this, the stiffness matrix can be obtained using the conventional variational formulation [DAW 84] as

$$\mathbf{K}_e = EI\int_0^{\ell_e} \frac{d^2\mathbf{N}(x)}{dx^2}\frac{d^2\mathbf{N}^T(x)}{dx^2}\mathrm{d}x = \frac{EI}{\ell_e^3}\begin{bmatrix} 12 & 6\ell_e & -12 & 6\ell_e \\ 6\ell_e & 4\ell_e^2 & -6\ell_e & 2\ell_e^2 \\ -12 & -6\ell_e & 12 & -6\ell_e^2 \\ 6\ell_e & 2\ell_e^2 & -6\ell_e & 4\ell_e^2 \end{bmatrix} \tag{8.8}$$

The mass matrix for the nonlocal element can be obtained as

$$\begin{aligned}\mathbf{M}_e &= m\int_0^{\ell_e} \mathbf{N}(x)\mathbf{N}^T(x)\mathrm{d}x + m(e_0a)^2\int_0^{\ell_e} \frac{d\mathbf{N}(x)}{dx}\frac{d\mathbf{N}^T(x)}{dx}\mathrm{d}x \\ &= \frac{m\ell_e}{420}\begin{bmatrix} 156 & 22\ell_e & 54 & -13\ell_e \\ 22\ell_e & 4\ell_e^2 & 13\ell_e & -3\ell_e^2 \\ 54 & 13\ell_e & 156 & -22\ell_e \\ -13\ell_e & -3\ell_e^2 & -22\ell_e & 4\ell_e^2 \end{bmatrix} + \left(\frac{e_0a}{\ell_e}\right)^2\frac{m\ell_e}{30}\begin{bmatrix} 36 & 3\ell_e & -36 & 3\ell_e \\ 3\ell_e & 4\ell_e^2 & -3\ell_e & -\ell_e^2 \\ -36 & -3\ell_e & 36 & -3\ell_e \\ 3\ell_e & -\ell_e^2 & -3\ell_e & 4\ell_e^2 \end{bmatrix}\end{aligned} \tag{8.9}$$

For the special case when the beam is local, the mass matrix derived above reduces to the classical mass matrix [PET 98, DAW 84] as $e_0a = 0$.

8.2.3. *Transverse vibration of nanoplates*

For the transverse bending vibration of a nonlocal damped thin plate, the equation of motion can be expressed by

$$\begin{aligned}&D\nabla^4 V(x,y,t) + m\left(1-(e_0a)^2\nabla^2\right)\left\{\frac{\partial^2 V(x,y,t)}{\partial t^2}\right\} + \widehat{c}_1\left(1-(e_0a)_1^2\nabla^2\right)\nabla^4\frac{\partial V(x,y,t)}{\partial x^4\partial t} \\ &\qquad + \widehat{c}_2\left(1-(e_0a)_2^2\nabla^2\right)\frac{\partial V(x,y,t)}{\partial t} = \left(1-(e_0a)^2\nabla^2\right)\{F(x,y,t)\}\end{aligned} \tag{8.10}$$

In the above equation $\nabla^2 = \left(\frac{\partial^2}{\partial x^2} + \frac{\partial^2}{\partial x^2}\right)$ is the differential operator, $D = \frac{Eh^3}{12(1-\nu^2)}$ is the bending rigidity, h is the thickness, ν is the Poisson's ratio, m is mass per unit area, e_0a is the nonlocal parameter, $V(x,y,t)$ is the transverse displacement and $F(x,y,t)$ is the applied force. The constant $\widehat{c}_1$ is the strain-rate-dependent viscous damping coefficient and $\widehat{c}_2$ is the velocity-dependent viscous damping coefficient. The damping nonlocal parameters are assumed to be zero for simplicity as before. We consider an element of dimension $2c \times 2b$ with bending stiffness D and mass per unit area m. An element of the plate is shown in Figure 8.3 together with the local coordinate system. The shape function matrix for the bending deformation is a 12×1 vector [DAW 84] and can be expressed as

$$\mathbf{N}(x,y) = \mathbf{C}_e^{-1}\boldsymbol{\alpha}(x,y) \tag{8.11}$$

Here the vector of polynomials is given by

$$\boldsymbol{\alpha}(x,y) = \begin{bmatrix} 1 & x & y & x^2 & xy & y^2 & x^3 & x^2y & xy^2 & y^3 & x^3y & xy^3 \end{bmatrix}^T \tag{8.12}$$

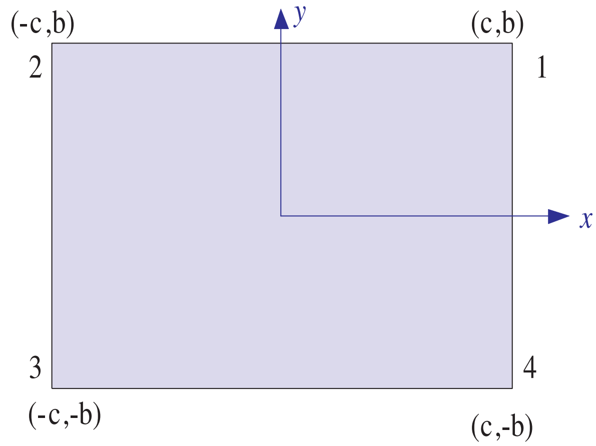

Figure 8.3 – A nonlocal element for the bending vibration of a plate. It has four nodes and twelve degrees of freedom. The displacement field within the element is expressed by cubic shape functions in both directions.

and the coefficient matrix can be obtained as

$$\mathbf{C}_e{}^{-1} = \frac{1}{8a^3b^3}\times$$
$$\begin{bmatrix} 2c^3b^3 & c^3b^4 & c^4b^3 & 2c^3b^3 & c^3b^4 & -b^3c^4 & 2c^3b^3 & -c^3b^4 & -c^4b^3 & 2c^3b^3 & -c^3b^4 & c^4b^3 \\ -3c^2b^3 & -c^2b^4 & -c^3b^3 & 3c^2b^3 & c^2b^4 & -c^3b^3 & 3c^2b^3 & -c^2b^4 & -c^3b^3 & -3c^2b^3 & c^2b^4 & -c^3b^3 \\ -3c^3b^2 & -c^3b^3 & -c^4b^2 & -3c^3b^2 & -c^3b^3 & c^4b^2 & 3c^3b^2 & -c^3b^3 & -c^4b^2 & 3c^3b^2 & -c^3b^3 & c^4b^2 \\ 0 & 0 & -c^2b^3 & 0 & 0 & c^2b^3 & 0 & 0 & c^2b^3 & 0 & 0 & -c^2b^3 \\ 4c^2b^2 & c^2b^3 & c^3b^2 & -4c^2b^2 & -c^2b^3 & c^3b^2 & 4c^2b^2 & -c^2b^3 & -c^3b^2 & -4c^2b^2 & c^2b^3 & -c^3b^2 \\ 0 & -c^3b^2 & 0 & 0 & -c^3b^2 & 0 & 0 & c^3b^2 & 0 & 0 & c^3b^2 & 0 \\ b^3 & 0 & cb^3 & -b^3 & 0 & cb^3 & -b^3 & 0 & cb^3 & b^3 & 0 & cb^3 \\ 0 & 0 & c^2b^2 & 0 & 0 & -c^2b^2 & 0 & 0 & c^2b^2 & 0 & 0 & -c^2b^2 \\ 0 & c^2b^2 & 0 & 0 & -c^2b^2 & 0 & 0 & c^2b^2 & 0 & 0 & -c^2b^2 & 0 \\ c^3 & c^3b & 0 & c^3 & c^3b & 0 & -c^3 & c^3b & 0 & -c^3 & c^3b & 0 \\ -b^2 & 0 & -cb^2 & b^2 & 0 & -cb^2 & -b^2 & 0 & cb^2 & b^2 & 0 & cb^2 \\ -c^2 & -c^2b & 0 & c^2 & c^2b & 0 & -c^2 & c^2b & 0 & c^2 & -c^2b & 0 \end{bmatrix} \quad (8.13)$$

Using the shape functions in Eq. (8.11), the stiffness matrix can be obtained using the conventional variational formulation [DAW 84] as

$$\mathbf{K}_e = \int_{A_e} \mathbf{B}^T\mathbf{E}\mathbf{B}\mathrm{d}A_e \quad (8.14)$$

In the preceding equation $\mathbf{B}$ is the strain-displacement matrix, and the matrix $\mathbf{E}$ is given by

$$\mathbf{E} = D\begin{bmatrix} 1 & \nu & 0 \\ \nu & 1 & 0 \\ 0 & 0 & \frac{1-\nu}{2} \end{bmatrix} \quad (8.15)$$

Evaluating the integral in Eq. (8.14), we can obtain the element stiffness matrix in closed-form as

$$\mathbf{K}_e = \frac{Eh^3}{12(1-\nu^2)}\mathbf{C}^{-1^T}\mathbf{k}_e\mathbf{C}^{-1} \quad (8.16)$$

where

$$\mathbf{k}_e = \begin{bmatrix} 0 & & & & & & & & & & & \\ 0 & 0 & & & & & & & & & & \\ 0 & 0 & 0 & & & & & & & & & \\ 0 & 0 & 0 & k_{e_{44}} & & & & & & & & \\ 0 & 0 & 0 & 0 & k_{e_{55}} & & & & & & & \\ 0 & 0 & 0 & k_{e_{64}} & 0 & k_{e_{66}} & & & & \text{symmetric} & & \\ 0 & 0 & 0 & 0 & 0 & 0 & k_{e_{77}} & & & & & \\ 0 & 0 & 0 & 0 & 0 & 0 & 0 & k_{e_{88}} & & & & \\ 0 & 0 & 0 & 0 & 0 & 0 & k_{e_{97}} & 0 & k_{e_{99}} & & & \\ 0 & 0 & 0 & 0 & 0 & 0 & 0 & k_{e_{10\,8}} & 0 & k_{e_{10\,10}} & & \\ 0 & 0 & 0 & 0 & k_{e_{11\,5}} & 0 & 0 & 0 & 0 & 0 & k_{e_{11\,11}} & \\ 0 & 0 & 0 & 0 & k_{e_{12\,5}} & 0 & 0 & 0 & 0 & 0 & k_{e_{12\,11}} & k_{e_{12\,12}} \end{bmatrix} \tag{8.17}$$

with

$$k_{e_{44}} = 16cb \qquad k_{e_{55}} = 8cb(1-\nu) \qquad k_{e_{64}} = 16\nu cb$$

$$k_{e_{66}} = 16cb \qquad k_{e_{77}} = 48c^3b \qquad k_{e_{88}} = \frac{16cb\left((2-2\nu)\,c^2 + b^2\right)}{3}$$

$$k_{e_{97}} = 16\nu c^3 b \qquad k_{e_{99}} = \frac{16cb(c^2 + 2(1-\nu)b^2)}{3} \qquad k_{e_{10\,8}} = 16\nu cb^2$$

$$k_{e_{10\,10}} = 48cb^3 \qquad k_{e_{11\,5}} = 8\,(1-\nu)\,c^3b \qquad k_{e_{11\,11}} = 4c^3b(\frac{9(1-\nu)c^2}{5} + 4b^2)$$

$$k_{e_{12\,5}} = 8\,(1-\nu)\,cb^3 \qquad k_{e_{12\,11}} = 8(\nu+1)c^3b^3 \qquad k_{e_{12\,12}} = \frac{8\,cb^3\left(10c^2 + 9(1-\nu)b^2\right)}{5}$$

The mass matrix for the nonlocal element can be obtained as

$$\begin{aligned} \mathbf{M}_e &= \rho h \int_{A_e} \left\{ \mathbf{N}(x,y)\mathbf{N}^T(x,y) + (e_0 a)^2 \left(\frac{\partial \mathbf{N}(x,y)}{\partial x} \frac{d\mathbf{N}^T(x,y)}{dx} + \frac{\partial \mathbf{N}(x,y)}{\partial x} \frac{d\mathbf{N}^T(x,y)}{dx} \right) \right\} \mathrm{d}A_e \\ &= \mathbf{M}_{0_e} + \left(\frac{e_0 a}{c}\right)^2 \mathbf{M}_{x_e} + \left(\frac{e_0 a}{b}\right)^2 \mathbf{M}_{y_e} \end{aligned} \tag{8.18}$$

The three matrices appearing in the above expression can be obtained in closed-form as

$$\mathbf{M}_{0_e} = \frac{\rho h c b}{3150} \times$$

$$\begin{bmatrix} 1727 & 461b & 461c & 613 & 199b & -274c & 197 & -116b & -116c & 613 & -274b & 199c \\ 461b & 160b^2 & 126cb & 199b & 80b^2 & -84cb & 116b & -60b^2 & -56cb & 274b & -120b^2 & 84cb \\ 461c & 126cb & 160c^2 & 274c & 84cb & -120c^2 & 116c & -56cb & -60c^2 & 199c & -84cb & 80c^2 \\ 613 & 199b & 274c & 1727 & 461b & -461c & 613 & -274b & -199c & 197 & -116b & 116c \\ 199b & 80b^2 & 84cb & 461b & 160b^2 & -126cb & 274b & -120b^2 & -84cb & 116b & -60b^2 & 56cb \\ -274c & -84cb & -120c^2 & -461c & -126cb & 160c^2 & -199c & 84cb & 80c^2 & -116c & 56cb & -60c^2 \\ 197 & 116b & 116c & 613 & 274b & -199c & 1727 & -461b & -461c & 613 & -199b & 274c \\ -116b & -60b^2 & -56cb & -274b & -120b^2 & 84cb & -461b & 160b^2 & 126cb & -199b & 80b^2 & -84cb \\ -116c & -56cb & -60c^2 & -199c & -84cb & 80c^2 & -461c & 126cb & 160c^2 & -274c & 84cb & -120c^2 \\ 613 & 274b & 199c & 197 & 116b & -116c & 613 & -199b & -274c & 1727 & -461b & 461c \\ -274b & -120b^2 & -84cb & -116b & -60b^2 & 56cb & -199b & 80b^2 & 84cb & -461b & 160b^2 & -126cb \\ 199c & 84cb & 80c^2 & 116c & 56cb & -60c^2 & 274c & -84cb & -120c^2 & 461c & -126cb & 160c^2 \end{bmatrix} \tag{8.19}$$

$$\mathbf{M}_{x_e} = \frac{\rho hcb}{630} \times$$
$$\begin{bmatrix} 276 & 66b & 42c & -276 & -66b & 42c & -102 & 39b & 21c & 102 & -39b & 21c \\ 66b & 24b^2 & 0 & -66b & -24b^2 & 0 & -39b & 18b^2 & 0 & 39b & -18b^2 & 0 \\ 42c & 0 & 112c^2 & -42c & 0 & -28c^2 & -21c & 0 & -14c^2 & 21c & 0 & 56c^2 \\ -276 & -66b & -42c & 276 & 66b & -42c & 102 & -39b & -21c & -102 & 39b & -21c \\ -66b & -24b^2 & 0 & 66b & 24b^2 & 0 & 39b & -18b^2 & 0 & -39b & 18b^2 & 0 \\ 42c & 0 & -28c^2 & -42c & 0 & 112c^2 & -21c & 0 & 56c^2 & 21c & 0 & -14c^2 \\ -102 & -39b & -21c & 102 & 39b & -21c & 276 & -66b & -42c & -276 & 66b & -42c \\ 39b & 18b^2 & 0 & -39b & -18b^2 & 0 & -66b & 24b^2 & 0 & 66b & -24b^2 & 0 \\ 21c & 0 & -14c^2 & -21c & 0 & 56c^2 & -42c & 0 & 112c^2 & 42c & 0 & -28c^2 \\ 102 & 39b & 21c & -102 & -39b & 21c & -276 & 66b & 42c & 276 & -66b & 42c \\ -39b & -18b^2 & 0 & 39b & 18b^2 & 0 & 66b & -24b^2 & 0 & -66b & 24b^2 & 0 \\ 21c & 0 & 56c^2 & -21c & 0 & -14c^2 & -42c & 0 & -28c^2 & 42c & 0 & 112c^2 \end{bmatrix} \tag{8.20}$$

$$\mathbf{M}_{y_e} = \frac{\rho hcb}{630} \times$$
$$\begin{bmatrix} 276 & 42b & 66c & 102 & 21b & -39c & -102 & 21b & 39c & -276 & 42b & -66c \\ 42b & 112b^2 & 0 & 21b & 56b^2 & 0 & -21b & -14b^2 & 0 & -42b & -28b^2 & 0 \\ 66c & 0 & 24c^2 & 39c & 0 & -18c^2 & -39c & 0 & 18c^2 & -66c & 0 & -24c^2 \\ 102 & 21b & 39c & 276 & 42b & -66c & -276 & 42b & 66c & -102 & 21b & -39c \\ 21b & 56b^2 & 0 & 42b & 112b^2 & 0 & -42b & -28b^2 & 0 & -21b & -14b^2 & 0 \\ -39c & 0 & -18c^2 & -66c & 0 & 24c^2 & 66c & 0 & -24c^2 & 39c & 0 & 18c^2 \\ -102 & -21b & -39c & -276 & -42b & 66c & 276 & -42b & -66c & 102 & -21b & 39c \\ 21b & -14b^2 & 0 & 42b & -28b^2 & 0 & -42b & 112b^2 & 0 & -21b & 56b^2 & 0 \\ 39c & 0 & 18c^2 & 66c & 0 & -24c^2 & -66c & 0 & 24c^2 & -39c & 0 & -18c^2 \\ -276 & -42b & -66c & -102 & -21b & 39c & 102 & -21b & -39c & 276 & -42b & 66c \\ 42b & -28b^2 & 0 & 21b & -14b^2 & 0 & -21b & 56b^2 & 0 & -42b & 112b^2 & 0 \\ -66c & 0 & -24c^2 & -39c & 0 & 18c^2 & 39c & 0 & -18c^2 & 66c & 0 & 24c^2 \end{bmatrix} \tag{8.21}$$

For the special case when the plate is local, the mass matrix derived above reduces to the classical mass matrix as $e_0a = 0$ [DAW 84].

Based on the discussions in this section for all the three systems considered here, in general the element mass matrix of a nonlocal dynamic system can be expressed as

$$\mathbf{M}_e = \mathbf{M}_{0_e} + \mathbf{M}_{\mu_e} \tag{8.22}$$

Here $\mathbf{M}_{0_e}$ is the element stiffness matrix corresponding to the underlying local system and $\mathbf{M}_{\mu_e}$ is the additional term arising due to the nonlocal effect.

8.3. Modal analysis of nonlocal dynamical systems

Using the finite element formulation, the stiffness matrix of the local and nonlocal system turns out to be identical to each other. The mass matrix of the nonlocal system is however different from its equivalent local counterpart. Assembling the element matrices and applying the boundary conditions, following the usual procedure of the finite element method [ZIE 91] one obtains the global mass matrix as

$$\mathbf{M} = \mathbf{M}_0 + \mathbf{M}_\mu \tag{8.23}$$

In the above equation $\mathbf{M}_0$ is the usual global mass matrix arising in the conventional local system and $\mathbf{M}_\mu$ is matrix arising due to nonlocal nature of the systems. In general we can express this matrix by

$$\mathbf{M}_\mu = \left(\frac{e_0a}{L}\right)^2 \widehat{\mathbf{M}}_\mu \tag{8.24}$$

where $\widehat{\mathbf{M}}_\mu$ is a nonnegative definite matrix. The matrix $\mathbf{M}_\mu$ is therefore, a scale-dependent matrix and its influence reduces if the length of the system L is large compared to the parameter $e_0 a$. Majority of the current finite element software and other computational tools do not explicitly consider the nonlocal part of the mass matrix. For the design and analysis of future generation of nano electromechanical systems it is vitally important to consider the nonlocal influence. In this section we are interested in understanding the impact of the difference in the mass matrix on the dynamic characteristics of the system. In particular the following questions of fundamental interest have been addressed:

– Under what condition a nonlocal system possess classical local normal modes?

– How the vibration modes and frequencies of a nonlocal system can be understood in the light of the results from classical local systems?

By addressing these questions, it would be possible to extend conventional 'local' elasticity based finite element software to analyse nonlocal systems arising in the modelling of complex nanoscale built-up structures.

8.3.1. *Conditions for classical normal modes*

The equation of motion of a discretised nonlocal damped system with n degrees of freedom can be expressed as

$$[\mathbf{M}_0 + \mathbf{M}_\mu]\,\ddot{\mathbf{u}}(t) + \mathbf{C}\dot{\mathbf{u}}(t) + \mathbf{K}\mathbf{u}(t) = \mathbf{f}(t) \tag{8.25}$$

Here $\mathbf{u}(t) \in \mathbb{R}^n$ is the displacement vector, $\mathbf{f}(t) \in \mathbb{R}^n$ is the forcing vector, $\mathbf{K}, \mathbf{C} \in \mathbb{R}^{n\times n}$ are respectively the global stiffness and the viscous damping matrix. In general $\mathbf{M}_0$ and $\mathbf{M}_\mu$ are positive definite symmetric matrices, $\mathbf{C}$ and $\mathbf{K}$ are non-negative definite symmetric matrices. The equation of motion of corresponding local system is given by

$$\mathbf{M}_0\ddot{\mathbf{u}}_0(t) + \mathbf{C}\dot{\mathbf{u}}_0(t) + \mathbf{K}\mathbf{u}_0(t) = \mathbf{f}(t) \tag{8.26}$$

where $\mathbf{u}_0(t) \in \mathbb{R}^n$ is the local displacement vector. The natural frequencies ($\omega_j \in \mathbb{R}$) and the mode shapes ($\mathbf{x}_j \in \mathbb{R}^n$) of the corresponding undamped local system can be obtained by solving the matrix eigenvalue problem [MEI 97] as

$$\mathbf{K}\mathbf{x}_j = \omega_j^2 \mathbf{M}_0 \mathbf{x}_j, \quad \forall\, j = 1, 2, \ldots, n \tag{8.27}$$

The undamped local eigenvectors satisfy an orthogonality relationship over the local mass and stiffness matrices, that is

$$\mathbf{x}_k^T \mathbf{M}_0 \mathbf{x}_j = \delta_{kj} \tag{8.28}$$

$$\text{and} \quad \mathbf{x}_k^T \mathbf{K} \mathbf{x}_j = \omega_j^2 \delta_{kj}, \quad \forall\, k, j = 1, 2, \ldots, n \tag{8.29}$$

where δ_{kj} is the Kroneker delta function. We construct the local modal matrix

$$\mathbf{X} = [\mathbf{x}_1, \mathbf{x}_2, \ldots, \mathbf{x}_n] \in \mathbb{R}^n \tag{8.30}$$

The local modal matrix can be used to diagonalize the local system (8.26) provided the damping matrix $\mathbf{C}$ is simultaneously diagonalizable with $\mathbf{M}_0$ and $\mathbf{K}$. This condition, known as the proportional damping, originally introduced by Lord Rayleigh [RAY 77] in 1877, is still in wide use today. The mathematical condition for proportional damping can be obtained from the commutitative behaviour of the system matrices [CAU 65]. This can be expressed as

$$\mathbf{C}\mathbf{M}_0^{-1}\mathbf{K} = \mathbf{K}\mathbf{M}_0^{-1}\mathbf{C} \tag{8.31}$$

or equivalently $\mathbf{C} = \mathbf{M}_0 f(\mathbf{M}_0^{-1}\mathbf{K})$ as shown in [ADH 06].

Considering undamped nonlocal system and premultiplying the equation by $\mathbf{M}_0^{-1}$ we have

$$\left(\mathbf{I}_n + \mathbf{M}_0^{-1}\mathbf{M}_\mu\right)\ddot{\mathbf{u}}(t) + \left(\mathbf{M}_0^{-1}\mathbf{K}\right)\mathbf{u}(t) = \mathbf{M}_0^{-1}\mathbf{f}(t) \tag{8.32}$$

This system can be diagonalized by a similarity transformation which also diagonalise $\left(\mathbf{M}_0^{-1}\mathbf{K}\right)$ provided the matrices $\left(\mathbf{M}_0^{-1}\mathbf{M}_\mu\right)$ and $\left(\mathbf{M}_0^{-1}\mathbf{K}\right)$ commute. This implies that the condition for existence of classical local normal modes is

$$\left(\mathbf{M}_0^{-1}\mathbf{K}\right)\left(\mathbf{M}_0^{-1}\mathbf{M}_\mu\right) = \left(\mathbf{M}_0^{-1}\mathbf{M}_\mu\right)\left(\mathbf{M}_0^{-1}\mathbf{K}\right) \tag{8.33}$$

$$\text{or} \quad \mathbf{K}\mathbf{M}_0^{-1}\mathbf{M}_\mu = \mathbf{M}_\mu\mathbf{M}_0^{-1}\mathbf{K} \tag{8.34}$$

If the above condition is satisfied, then a nonlocal undamped system can be diagonalised by the classical local normal modes. However, it is also possible to have nonlocal normal modes which can diagonalize the nonlocal undamped system as discussed in the next subsection.

8.3.2. *Nonlocal normal modes*

Nonlocal normal modes can be obtained by the undamped nonlocal eigenvalue problem

$$\mathbf{K}\mathbf{u}_j = \lambda_j^2\left[\mathbf{M}_0 + \mathbf{M}_\mu\right]\mathbf{u}_j, \quad \forall\, j = 1, 2, \ldots, n \tag{8.35}$$

Here λ_j and $\mathbf{u}_j$ are the nonlocal natural frequencies and nonlocal normal modes of the system. We can define a nonlocal modal matrix

$$\mathbf{U} = [\mathbf{u}_1, \mathbf{u}_2, \ldots, \mathbf{u}_n] \in \mathbb{R}^n \tag{8.36}$$

which will unconditionally diagonalize the nonlocal undamped system. It should be remembered that in general nonlocal normal modes and frequencies will be different from their local counterparts.

Under certain restrictive condition it may be possible to diagonalise the damped nonlocal system using classical normal modes. Premultiplying the equation of motion (8.25) by $\mathbf{M}_0^{-1}$, the required condition is that $\left(\mathbf{M}_0^{-1}\mathbf{M}_\mu\right)$, $\left(\mathbf{M}_0^{-1}\mathbf{C}\right)$ and $\left(\mathbf{M}_0^{-1}\mathbf{K}\right)$ must commute pairwise. This implies that in addition to the two conditions given by Eqs. (8.31) and (8.34), we also need a third condition

$$\mathbf{C}\mathbf{M}_0^{-1}\mathbf{M}_\mu = \mathbf{M}_\mu\mathbf{M}_0^{-1}\mathbf{C} \tag{8.37}$$

If we consider the diagonalization of the nonlocal system by the nonlocal modal matrix in (8.36), then the concept of proportional damping can be applied similar to that of the local system. One can obtain the required condition similar to Caughey's condition [CAU 65] as in Eq. (8.31) by replacing the mass matrix with $\mathbf{M}_0 + \mathbf{M}_\mu$. If this condition is satisfied, then the equation of motion can be diagonalised by the nonlocal normal modes and in general not by the classical normal modes.

8.3.3. *Approximate nonlocal normal modes*

Majority of the existing finite element software calculate the classical normal modes. However, it was shown that only under certain restrictive condition, the classical normal modes can be used to diagonalise the system. In general one need to use nonlocal normal modes to diagonalise the equation of motion (8.25), which is necessary for efficient dynamic analysis and physical understanding of the system. In this section we aim to express nonlocal normal modes in terms of classical normal modes. Since the classical normal modes are well understood, this approach will allow us to develop physical understanding of the nonlocal normal modes.

For distinct undamped eigenvalues (ω_l^2), local eigenvectors $\mathbf{x}_l$, $\forall\, l = 1, \ldots, n$, form a complete set of vectors. For this reason each nonlocal normal mode $\mathbf{u}_j$ can be expanded as a linear combination of $\mathbf{x}_l$. Thus, an expansion of the form

$$\mathbf{u}_j = \sum_{l=1}^{n} \alpha_l^{(j)}\mathbf{x}_l \tag{8.38}$$

may be considered. Without any loss of generality, we can assume that $\alpha_j^{(j)} = 1$ (normalization) which leaves us to determine $\alpha_l^{(j)}, \forall l \neq j$. Substituting the expansion of $\mathbf{u}_j$ into the eigenvalue equation (8.35), one obtains

$$\left[-\lambda_j^2 \left(\mathbf{M}_0 + \mathbf{M}_\mu\right) + \mathbf{K}\right] \sum_{l=1}^{n} \alpha_l^{(j)} \mathbf{x}_l = \mathbf{0} \tag{8.39}$$

For the case when $\alpha_l^{(j)}$ are approximate, the error involving the projection in Eq. (8.38) can be expressed as

$$\boldsymbol{\varepsilon}_j = \sum_{l=1}^{n} \left[-\lambda_j^2 \left(\mathbf{M}_0 + \mathbf{M}_\mu\right) + \mathbf{K}\right] \alpha_l^{(j)} \mathbf{x}_l \tag{8.40}$$

We use a Galerkin approach to minimise this error by viewing the expansion as a projection in the basis functions $\mathbf{x}_l \in \mathbb{R}^n, \forall l = 1, 2, \ldots n$. Therefore, making the error orthogonal to the basis functions one has

$$\boldsymbol{\varepsilon}_j \perp \mathbf{x}_l \quad \text{or} \quad \mathbf{x}_k^T \boldsymbol{\varepsilon}_j = 0 \quad \forall\ k = 1, 2, \ldots, n \tag{8.41}$$

Using the orthogonality property of the undamped local modes described by Eqs. (8.28) and (8.29) one obtains

$$\sum_{l=1}^{n} \left[-\lambda_j^2 \left(\delta_{kl} + M'_{\mu_{kl}}\right) + \omega_k^2 \delta_{kl}\right] \alpha_l^{(j)} = 0 \tag{8.42}$$

where $M'_{\mu_{kl}} = \mathbf{x}_k^T \mathbf{M}_\mu \mathbf{x}_l$ are the elements of the nonlocal part of the modal mass matrix. The j-th equation of this set obtained by setting $k = j$ and can be written as

$$-\lambda_j^2 \left(1 + M'_{\mu_{jj}}\right) + \omega_j^2 - \lambda_j^2 \sum_{l \neq j}^{n} \left(M'_{\mu_{jl}}\right) \alpha_l^{(j)} = 0 \tag{8.43}$$

Assuming the off-diagonal terms of the nonlocal part of the modal mass matrix are small and $\alpha_l^{(j)} \ll 1, \forall l \neq j$, approximate nonlocal frequencies can be obtained as

$$\lambda_j \approx \frac{\omega_j}{\sqrt{1 + M'_{\mu_{jj}}}} \tag{8.44}$$

This important equation gives an explicit closed-form expression relating nonlocal natural frequencies λ_j and local natural frequencies ω_j. If the length-scale parameter is large, then diagonal elements of the nonlocal part of the modal mass matrix becomes smaller and consequently the nonlocal frequencies approach the classical local frequencies. Equation (8.44) can also be viewed as a general correction to the local frequencies due to the nonlocal effect arising due to small length scale.

For the general case when $k \neq j$, from Eq. (8.42) we have

$$\left[-\lambda_j^2 \left(1 + M'_{\mu_{kk}}\right) + \omega_k^2\right] \alpha_k^{(j)} - \lambda_j^2 \sum_{l \neq k}^{n} \left(M'_{\mu_{kl}}\right) \alpha_l^{(j)} = 0 \tag{8.45}$$

Recalling that $\alpha_j^{(j)} = 1$, this equation can be expressed as

$$\left[-\lambda_j^2 \left(1 + M'_{\mu_{kk}}\right) + \omega_k^2\right] \alpha_k^{(j)} = \lambda_j^2 \left[M'_{\mu_{kj}} + \sum_{l \neq k \neq j}^{n} M'_{\mu_{kl}} \alpha_l^{(j)}\right] \tag{8.46}$$

Again assuming the off-diagonal terms of the nonlocal part of the modal mass matrix are small and $\alpha_l^{(j)} \ll 1, \forall l \neq j$, we can obtain

$$\alpha_k^{(j)} \approx \frac{\lambda_j^2 M'_{\mu_{kj}}}{-\lambda_j^2\left(1+M'_{\mu_{kk}}\right)+\omega_k^2} = \frac{\lambda_j^2}{\left(\lambda_k^2-\lambda_j^2\right)}\frac{M'_{\mu_{kj}}}{\left(1+M'_{\mu_{kk}}\right)} \tag{8.47}$$

Substituting this in the original expansion (8.38), the nonlocal normal modes can be expressed in terms of the classical normal modes as

$$\mathbf{u}_j \approx \mathbf{x}_j + \sum_{k\neq j}^{n} \frac{\lambda_j^2}{\left(\lambda_k^2-\lambda_j^2\right)}\frac{M'_{\mu_{kj}}}{\left(1+M'_{\mu_{kk}}\right)}\mathbf{x}_k \tag{8.48}$$

This equation explicitly relates nonlocal normal modes with the classical normal modes. From this expression, the following insights about the nonlocal normal modes can be deduced

– Each nonlocal mode can be viewed as a sum of two principal components. One of them is parallel to the corresponding local mode and the other is orthogonal to it as all $\mathbf{x}_k$ are orthogonal to $\mathbf{x}_j$ for $j \neq k$.

– Due to the term $\left(\lambda_k^2-\lambda_j^2\right)$ in the denominator, for a given nonlocal mode, only few adjacent local modes contributes to the orthogonal component.

– For systems with well separated natural frequencies, the contribution of the orthogonal component becomes smaller compared to the parallel component.

Equations (8.44) and (8.48) completely defines the nonlocal natural frequencies and mode shapes in terms of the local natural frequencies and mode shapes. Accuracy of these expressions will be investigated through numerical examples in section 8.5. Dynamic response of nonlocal damped systems is considered next.

8.4. Dynamics of damped nonlocal systems

Forced response of damped nonlocal systems in the frequency domain is considered. Assuming all the initial conditions are zero and taking the Fourier transformation of the equation of motion (8.25) we have

$$\mathbf{D}(\mathrm{i}\omega)\bar{\mathbf{u}}(\mathrm{i}\omega) = \bar{\mathbf{f}}(\mathrm{i}\omega) \tag{8.49}$$

where the nonlocal dynamic stiffness matrix is given by

$$\mathbf{D}(\mathrm{i}\omega) = -\omega^2\left[\mathbf{M}_0+\mathbf{M}_\mu\right] + \mathrm{i}\omega\mathbf{C} + \mathbf{K} \tag{8.50}$$

In Eq. (8.49) $\bar{\mathbf{u}}(\mathrm{i}\omega)$ and $\bar{\mathbf{f}}(\mathrm{i}\omega)$ are respectively the Fourier transformations of the response and the forcing vectors. Using the local modal matrix (8.30), the dynamic stiffness matrix can be transformed to the modal coordinate as

$$\mathbf{D}'(\mathrm{i}\omega) = \mathbf{X}^T\mathbf{D}(\mathrm{i}\omega)\mathbf{X} = -\omega^2\left[\mathbf{I}+\mathbf{M}'_\mu\right] + \mathrm{i}\omega\mathbf{C}' + \mathbf{\Omega}^2 \tag{8.51}$$

where $\mathbf{I}$ is a n-dimensional identity matrix, $\mathbf{\Omega}^2$ is a diagonal matrix containing the squared local natural frequencies and $(\bullet)'$ denotes that the quantity is in the modal coordinates. Unless all the conditions derived in subsection 8.3.2 are satisfied, in general $\mathbf{M}'_\mu$ and $\mathbf{C}'$ are not diagonal matrices. We separate the diagonal and off-diagonal terms of these matrices and rewrite Eq. (8.51) as

$$\mathbf{D}'(\mathrm{i}\omega) = \underbrace{-\omega^2\left[\mathbf{I}+\overline{\mathbf{M}}'_\mu\right] + \mathrm{i}\omega\overline{\mathbf{C}}' + \mathbf{\Omega}^2}_{\text{diagonal}} + \underbrace{\left(-\omega^2\Delta\mathbf{M}'_\mu + \mathrm{i}\omega\Delta\mathbf{C}'\right)}_{\text{off-diagonal}} \tag{8.52}$$

$$= \overline{\mathbf{D}}'(\mathrm{i}\omega) + \Delta\mathbf{D}'(\mathrm{i}\omega) \tag{8.53}$$

From Eq. (8.49) the dynamic response of the system can be obtained as

$$\bar{\mathbf{u}}(\mathrm{i}\omega) = \mathbf{H}(\mathrm{i}\omega)\bar{\mathbf{f}}(\mathrm{i}\omega) = \left[\mathbf{X}\mathbf{D}'^{-1}(\mathrm{i}\omega)\mathbf{X}^T\right]\bar{\mathbf{f}}(\mathrm{i}\omega) \tag{8.54}$$

where the matrix $\mathbf{H}(\mathrm{i}\omega)$ is known as the transfer function matrix. From the expression of the modal dynamic stiffness matrix in Eq. (8.53) we have

$$\mathbf{D}^{'^{-1}}(\mathrm{i}\omega) = \left[\overline{\mathbf{D}}'(\mathrm{i}\omega)\left(\mathbf{I}+\overline{\mathbf{D}}^{'^{-1}}(\mathrm{i}\omega)\Delta\mathbf{D}'(\mathrm{i}\omega)\right)\right]^{-1} \tag{8.55}$$

$$\approx \overline{\mathbf{D}}^{'^{-1}}(\mathrm{i}\omega) - \overline{\mathbf{D}}^{'^{-1}}(\mathrm{i}\omega)\Delta\mathbf{D}'(\mathrm{i}\omega)\overline{\mathbf{D}}^{'^{-1}}(\mathrm{i}\omega) \tag{8.56}$$

In the above equation the diagonal part $\overline{\mathbf{D}}^{'^{-1}}(\mathrm{i}\omega)$ is expected to be the dominant term and its elements can be expressed as

$$\left\{\overline{\mathbf{D}}^{'^{-1}}(\mathrm{i}\omega)\right\}_{jj} = \frac{1}{-\omega^2\left(1+M'_{\mu_{jj}}\right)+2\mathrm{i}\omega\omega_j\zeta_j+\omega_j^2} \tag{8.57}$$

In the above we defined the modal damping factors as

$$\left\{\overline{\mathbf{C}}'\right\}_{jj} = 2\omega_j\zeta_j \tag{8.58}$$

Substituting the approximate expression of $\mathbf{D}^{'^{-1}}(\mathrm{i}\omega)$ from Eq. (8.56) into the expression of the transfer function matrix in Eq. (8.54) we have

$$\mathbf{H}(\mathrm{i}\omega) = \left[\mathbf{X}\mathbf{D}^{'^{-1}}(\mathrm{i}\omega)\mathbf{X}^T\right] \approx \overline{\mathbf{H}}'(\mathrm{i}\omega) - \Delta\mathbf{H}'(\mathrm{i}\omega) \tag{8.59}$$

where

$$\overline{\mathbf{H}}'(\mathrm{i}\omega) = \mathbf{X}\overline{\mathbf{D}}'(\mathrm{i}\omega)\mathbf{X}^T = \sum_{k=1}^{n}\frac{\mathbf{x}_k\mathbf{x}_k^T}{-\omega^2\left(1+M'_{\mu_{kk}}\right)+2\mathrm{i}\omega\omega_k\zeta_k+\omega_k^2} \tag{8.60}$$

$$\text{and}\quad \Delta\mathbf{H}'(\mathrm{i}\omega) = \mathbf{X}\overline{\mathbf{D}}^{'^{-1}}(\mathrm{i}\omega)\Delta\mathbf{D}'(\mathrm{i}\omega)\overline{\mathbf{D}}^{'^{-1}}(\mathrm{i}\omega)\mathbf{X}^T \tag{8.61}$$

Considering that the matrix $\Delta\mathbf{D}'(\mathrm{i}\omega)$ has only off-diagonal terms, expanding the matrix multiplications a general term of the previous matrix can be expressed as

$$\Delta H'_{ij}(\mathrm{i}\omega) = \sum_{l=1}^{n}\sum_{k\neq l}^{n}\frac{x_{il}\Delta D'_{lk}(\mathrm{i}\omega)x_{jk}}{\left(-\omega^2(1+M'_{\mu_{ll}})+2\mathrm{i}\omega\omega_l\zeta_l+\omega_l^2\right)\left(-\omega^2(1+M'_{\mu_{kk}})+2\mathrm{i}\omega\omega_k\zeta_k+\omega_k^2\right)} \tag{8.62}$$

Equation (8.59) therefore completely defines the transfer function of the damped nonlocal system in terms of the classical normal modes. This can be useful in practice as all the quantities arise in this expression can be obtained from a conventional finite element software. One only needs the nonlocal part of the mass matrix as derived in section 8.2. Some notable features of the expression of the approximate transfer function matrix in Eq. (8.59) are

– For lightly damped systems, from Eq. (8.60) observe that the transfer function will have peaks around the nonlocal natural frequencies derived in the previous section. This justifies the consistency of the approximation used in the paper.

– The decomposition in Eq. (8.52) indicates that error in the transfer function depends on two components. They include the off-diagonal part of the of the modal nonlocal mass matrix $\Delta\mathbf{M}'_\mu$ and the off-diagonal part of the of the modal damping matrix $\Delta\mathbf{C}'$. While the error in in the damping term is present for non proportionally damped local systems, the error due to the nonlocal modal mass matrix in unique to the nonlocal system.

– For a proportionally damped system $\Delta\mathbf{C}' = \mathbf{O}$. For this case error in the transfer function only depends on $\Delta\mathbf{M}'_\mu$.

– In general, error in the transfer function is expected to be higher for higher frequencies as both $\Delta\mathbf{C}'$ and $\Delta\mathbf{M}'_\mu$ are weighted by frequency ω.

The expressions of the nonlocal natural frequencies (8.44), nonlocal normal modes (8.48) and the nonlocal transfer function matrix (8.59) allow us to understand the dynamic characteristic of a nonlocal system in a qualitative and quantitative manner in the light of equivalent local systems. Next we illustrate these new expressions by numerical examples of nanoscale structures.

8.5. Numerical examples

8.5.1. *Axial vibration of a single-walled carbon nanotube*

A single-walled carbon nanotube (SWCNT) is considered to examine the accuracy of the nonlocal finite element formulation and approximate expressions of the natural frequencies, normal modes and transfer functions. A zigzag (7, 0) SWCNT with Young's modulus $E = 6.85$ TPa, $L = 25$nm, density $\rho = 9.517 \times 10^3$ kg/m^3 and thickness t = 0.08nm is taken from [MUR 11b]. The system considered here is shown in Figure 8.4. For a carbon

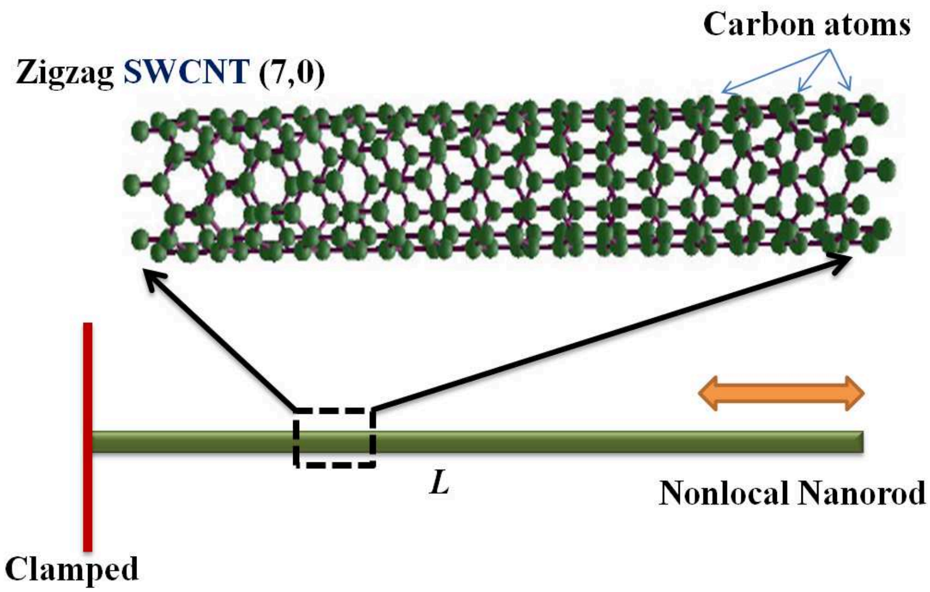

Figure 8.4 – Axial vibration of a zigzag (7, 0) single-walled carbon nanotube (SWCNT) with clamped-free boundary condition.

nanotube with chirality (n_i, m_i), the diameter can be given by

$$d_i = \frac{r}{\pi}\sqrt{n_i^2 + m_i^2 + n_i m_i} \tag{8.63}$$

where $r = 0.246$nm. The diameter of the SWCNT shown in Figure 8.4 is 0.55nm. A constant modal damping factor of 1% for all the modes is assumed. By comparing with MD simulation results [CHO 11a, CHO 10] it was observed that $e_0a = 1$ nm is the optimal value of the nonlocal parameter. In this study however we consider a range of values of e_0a within 0-2 nm to understand its role on the accuracy of the dynamic characteristics of the system.

We consider clamped-free boundary condition for the SWCNT. Undamped nonlocal natural frequencies can be obtained [AYD 09] as

$$\lambda_j = \sqrt{\frac{EA}{m}}\frac{\sigma_j}{\sqrt{1+\sigma_j^2(e_0a)^2}}, \quad \text{where} \quad \sigma_j = \frac{(2j-1)\pi}{2L}, \quad j = 1, 2, \cdots \tag{8.64}$$

EA is the axial rigidity and m is the mass per unit length of the SWCNT. For the finite element analysis the SWCNT is divided into 200 elements. The dimension of each of the system matrices become 200×200, that is $n = 200$. The global mass matrices $\mathbf{M}_0$ and $\mathbf{M}_\mu$ are obtained by assembling the element mass matrix given by (8.4). For this case it turns out (see element stiffness matrix in (8.3)) that the nonlocal part of the mass matrix is actually proportional to the stiffness matrix, that is $\mathbf{M}_\mu \propto \mathbf{K}$. Therefore, the condition for the existence of classical normal modes for the undamped system given by Eq. (8.34) is exactly satisfied in this case. This in turn implies that the error in the approximate expressions in subsection 8.3.2 should be zero as $M_{\mu_{kl}} = 0, \forall k \neq l$. We give numerical results to demonstrate that the theory for the existence of classical normal modes for nonlocal system derived in subsection 8.3.1 and the approximate expressions derived in subsection 8.3.2 are consistent.

In Figure 8.5, the natural frequencies obtained using the analytical expression (8.64) are compared with direct finite element simulation results. The frequency values are normalised with respect to the first local natural frequency ω_1. First 20 nonlocal natural frequencies are shown and four values of e_0a, namely 0.5, 1.0, 1.5 and 2.0nm

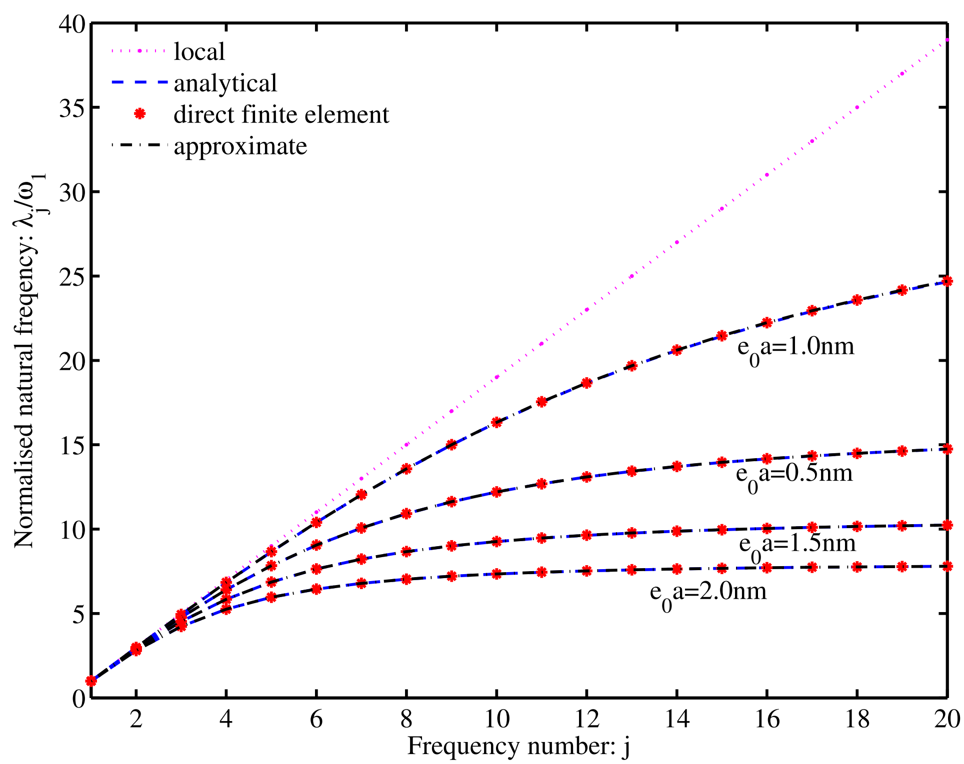

Figure 8.5 – The variation of first 20 undamped natural frequencies for the axial vibration of SWCNT. Four representative values of e_0a (in nm) are considered.

have been used. In the same figure, natural frequencies obtained using the direct finite element method and the results obtained using the approximate expression (8.44) are also shown. It can be observed that the values obtains using three different approaches coincide for this problem. Natural frequencies corresponding to the underlying local system is shown in Figure 8.5. Local frequencies are qualitatively different from nonlocal frequencies as it increases linearly with the number of modes. Nonlocal frequencies on the other hand approaches to a constant value with increasing modes. This upper bound is known as the asymptotic frequency [ADH 13] and given by $\lambda_{\max} = \frac{1}{(e_0a)}\sqrt{\frac{EA}{m}}$. It is worth noting that the approximate expression of the natural frequency given by Eq. (8.44) is able to capture the asymptotic frequency for the axial vibration of SWCNT. Therefore, Eq. (8.44) can be used to understand both quantitative and qualitative behaviour of the natural frequencies of a nonlocal system.

In Figure 8.6 mode shapes corresponding to modes 2, 5, 6 and 9 are shown for four values of the nonlocal parameter. These mode numbers are selected for illustration only. The results obtained from the direct finite

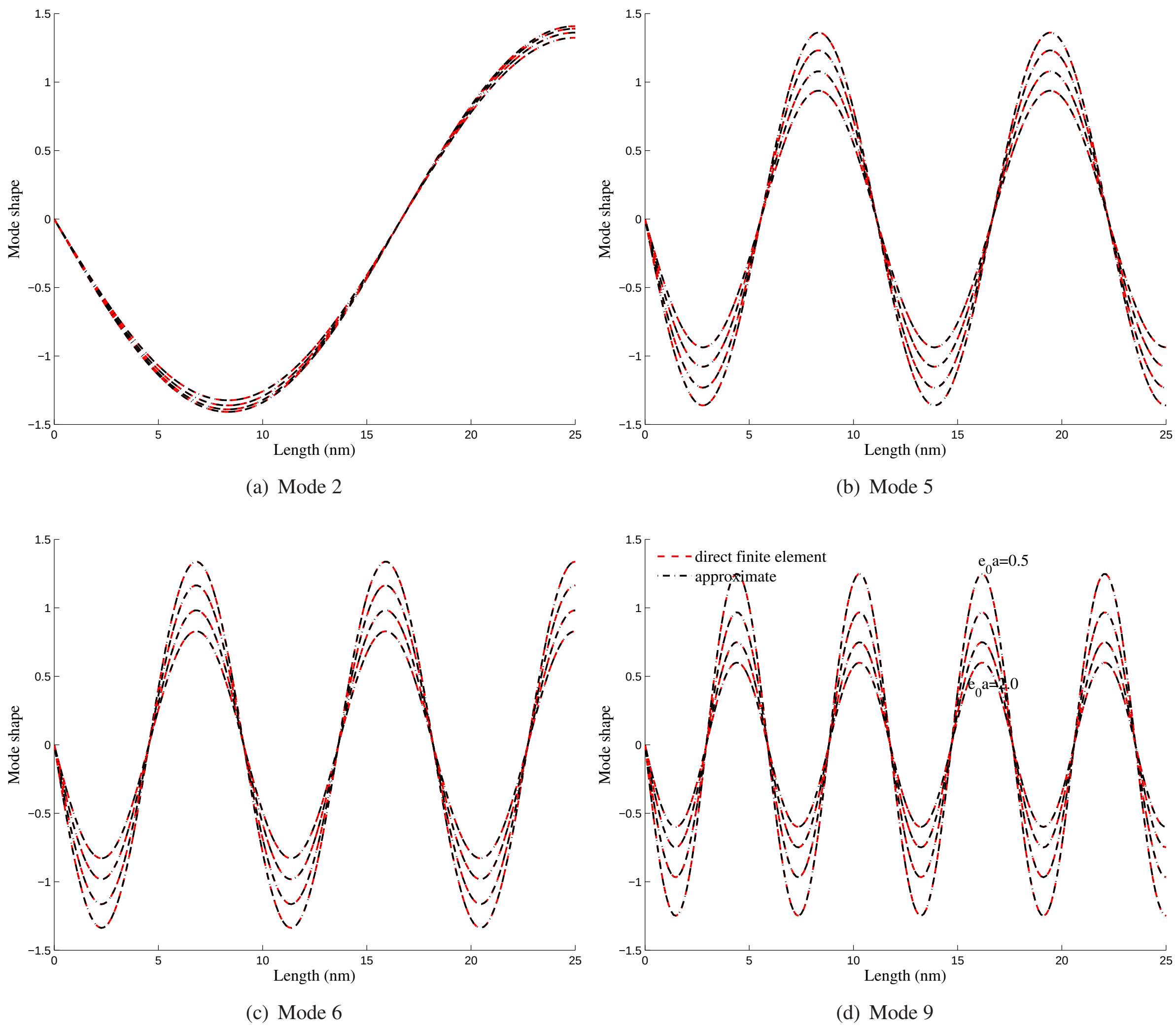

(a) Mode 2
(b) Mode 5
(c) Mode 6
(d) Mode 9

Figure 8.6 – Four selected mode shapes for the axial vibration of SWCNT. Exact finite element results are compared with the approximate analysis based on local eigensolutions. In each subplot four different values of e_0a, namely 0.5, 1.0, 1.5 and 2.0nm have been used (see subplot d).

element is compared with the approximate expression given by Eq. (8.48). The mode shapes obtained by both approaches agree each other well.

Finally in Figure 8.7 the frequency response function of the tip of the SWCNT is shown for the four representative values of the nonlocal parameter. In the x-axis, excitation frequency normalised with respect to the first local frequency is considered. The frequency response is normalised by the static response δ_{st} (response when the excitation frequency is zero). The frequency response function of the underlying local model is also plotted to show the difference between the local and nonlocal responses. For the nonlocal system, the frequency response is obtained by the direct finite element method and the approximation derived in section 8.4. As proportional damping model is assumed, the off-diagonal part of the modal damping matrix is a null matrix. For this case the approximate solution match exactly to the results obtained from the direct finite element method.

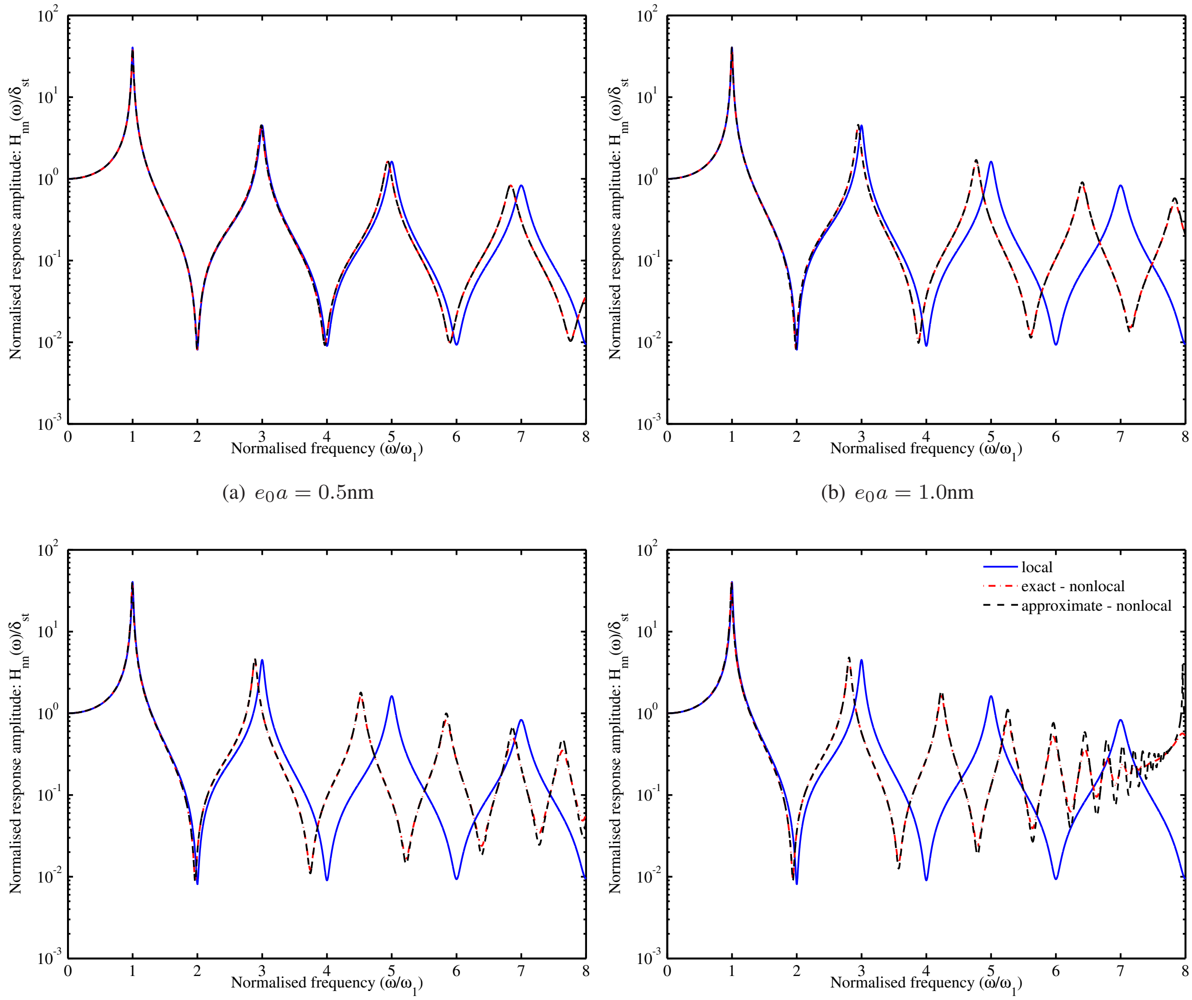

(a) $e_0a = 0.5$nm (b) $e_0a = 1.0$nm

(c) $e_0a = 1.5$nm (d) $e_0a = 2.0$nm

Figure 8.7 – Amplitude of the normalised frequency response of the SWCNT at the tip for different values of e_0a. Exact finite element results are compared with the approximate analysis based on local eigensolutions.

8.5.2. *Bending vibration of a double-walled carbon nanotube*

A double-walled carbon nanotube (DWCNT) is considered to examine the bending vibration characteristics. An armchair (5, 5), (8, 8) DWCNT with Young's modulus $E = 1.0$ TPa, $L = 30$ nm, density $\rho = 2.3 \times 10^3$ kg/m^3 and thickness t = 0.35 nm is considered as in [MUR 12b]. The inner and the outer diameters of the DWCNT are respectively 0.68nm and 1.1nm. The system considered here is shown in Figure 8.8 . We consider pinned-pinned boundary condition for the DWCNT. Undamped nonlocal natural frequencies can be obtained [AYD 09] as

$$\lambda_j = \sqrt{\frac{EI}{m}} \frac{\beta_j^2}{\sqrt{1+\beta_j^2(e_0a)^2}} \quad \text{where} \quad \beta_j = j\pi/L, \quad j = 1, 2, \cdots \tag{8.65}$$

EI is the bending rigidity and m is the mass per unit length of the DWCNT. For the finite element analysis the DWCNT is divided into 100 elements. The dimension of each of the system matrices become 200×200, that is $n = 200$. The global mass matrices $\mathbf{M}_0$ and $\mathbf{M}_\mu$ are obtains by assembling the element mass matrix given by

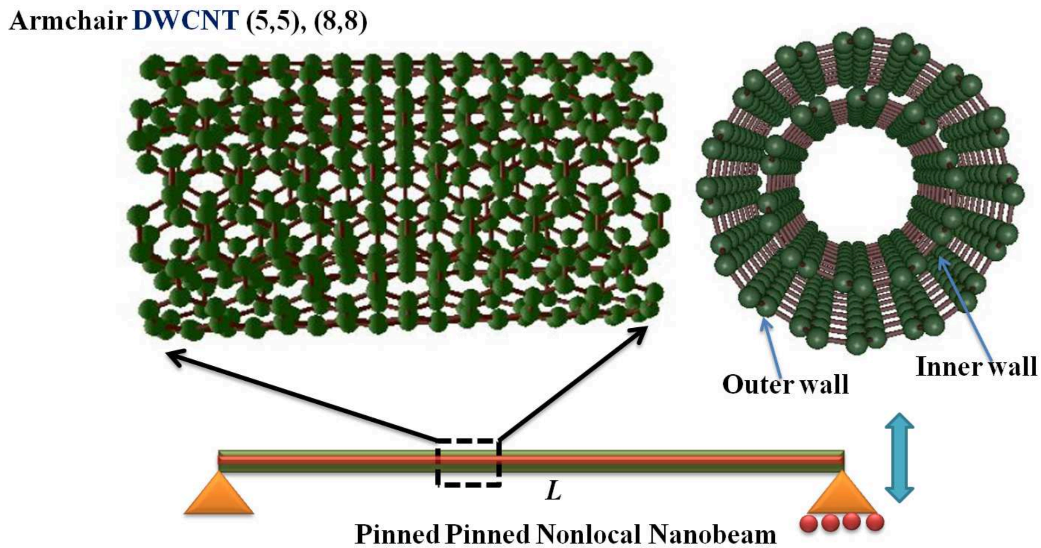

Figure 8.8 – Bending vibration of an armchair (5, 5), (8, 8) double-walled carbon nanotube (DWCNT) with pinned-pinned boundary condition.

(8.9). Unlike the case of the axial vibration of rods, the nonlocal part of the mass matrix is not proportional to the stiffness matrix. Therefore, the condition for the existence of classical normal modes for the undamped system given by Eq. (8.34) is not satisfied for this case. This numerical study therefore quantifies the accuracy of the approximate expression proposed in the paper.

The natural frequencies obtained using the analytical expression (8.65) are compared with direct finite element simulation in Figure 8.9. The frequency values are normalised with respect to the first local natural frequency. First 20 nonlocal natural frequencies are shown for four distinct values of e_0a, namely 0.5, 1.0, 1.5 and 2.0nm. In the same figure, natural frequencies obtained using the direct finite element method and the results obtained using the approximate expression (8.44) are also shown. It can be observed that the values obtains using three different approaches almost coincide for this problem. Natural frequencies corresponding to the underlying local system is shown in Figure 8.9. Local frequencies are qualitatively different from nonlocal frequencies as it increases quadratically with the number of modes. Nonlocal frequencies on the other hand increases linearly with the number of modes. The approximate expression of the natural frequency given by Eq. (8.44) is able to capture this crucial qualitative difference.

In Figure 8.10 mode shapes corresponding to mode 2, 5, 6 and 9 are shown for four values of the nonlocal parameter. These mode numbers are selected for illustration only. The results obtained from the direct finite element is compared with the approximate expression given by Eq. (8.48). The mode shapes obtain by both approach agree to each other.

In Figure 8.11 the amplitude of the frequency response function $H_{ij}(\omega)$ for $i = 6, j = 8$ is shown for the four representative values of the nonlocal parameter. In the x-axis, excitation frequency normalised with respect to the first local frequency is considered. The frequency response is normalise by the static response d_{st}. The frequency response function of the underlying local model is also plotted to show the difference between the local and nonlocal response. For the nonlocal system, the frequency response is obtained by the direct finite element method and the approximation derived in section 8.4. As proportional damping model is assumed, the off-diagonal part of the modal damping matrix is a null matrix. For this case the approximate solution match closely to the results obtained from the direct finite element method. The dynamic response of the nonlocal system becomes very different from the corresponding local system for higher frequency values and higher values of the nonlocal

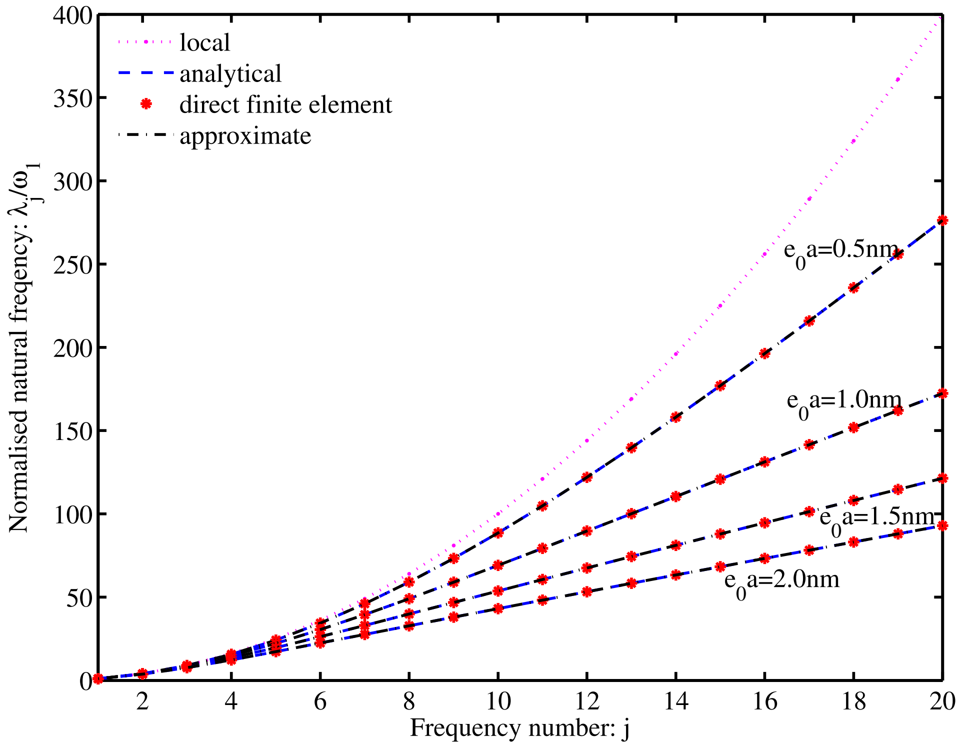

Figure 8.9 – The variation of first 20 undamped natural frequencies for the bending vibration of DWCNT. Four representative values of e_0a (in nm) are considered.

parameter e_0a. The proposed approximate expression of the transfer function given in Eq. (8.59) can be used to understand this significant different behaviour for the bending vibration of DWCNT.

8.5.3. *Transverse vibration of a single-layer graphene sheet*

A rectangular single-layer graphene sheet (SLGS) is considered to examine the transverse vibration characteristics of nanoplates. The graphene sheet is of dimension L=20nm, W=15nm and Young's modulus $E = 1.0$ TPa, density $\rho = 2.25 \times 10^3$ kg/m^3, Poisson's ratio $\nu = 0.3$ and thickness h = 0.34nm is considered as in [CHO 11b]. The system considered here is shown in Figure 8.12 . We consider simply supported boundary condition along the four edges for the SLGS. Undamped nonlocal natural frequencies can be obtained [KIA 11, KAR 10] as

$$\lambda_{ij} = \sqrt{\frac{D}{m}} \frac{\beta_{ij}^2}{\sqrt{1+\beta_{ij}^2(e_0a)^2}} \quad \text{where} \quad \beta_{ij} = \sqrt{(i\pi/L)^2 + (j\pi/W)^2},\ i,j = 1,2,\cdots \tag{8.66}$$

D is the bending rigidity and m is the mass per unit area of the SLGS. For the finite element analysis the DWCNT is divided into 20×15 elements. The dimension of each of the system matrices become 868×868, that is $n = 868$. The global mass matrices $\mathbf{M}_0$ and $\mathbf{M}_\mu$ are obtains by assembling the element mass matrix given by (8.18). Like the case of the bending vibration of nanobeams, the nonlocal part of the mass matrix is not proportional to the stiffness matrix. Therefore, the condition for the existence of classical normal modes for the undamped system given by Eq. (8.34) is not satisfied for this case. Among the three types of systems considered here, only the nanorod satisfy the condition of existence of classical normal modes.

In Figure 8.13, the natural frequencies obtained using the analytical expression (8.66) are compared with direct finite element simulation. The frequency values are normalised with respect to the first local natural frequency.

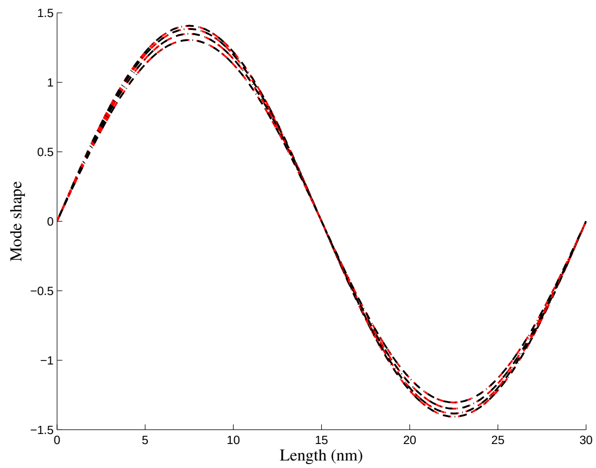

(a) Mode 2

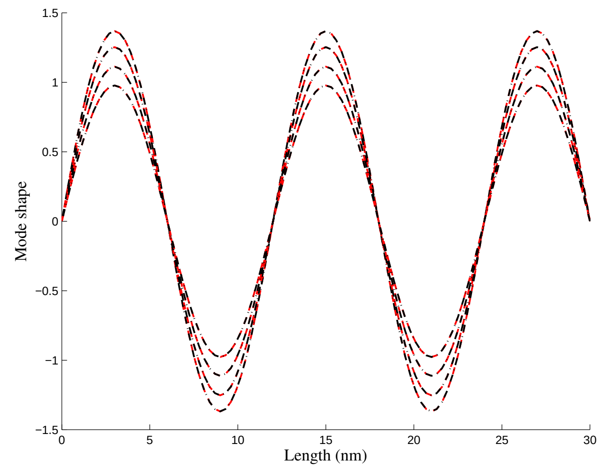

(b) Mode 5

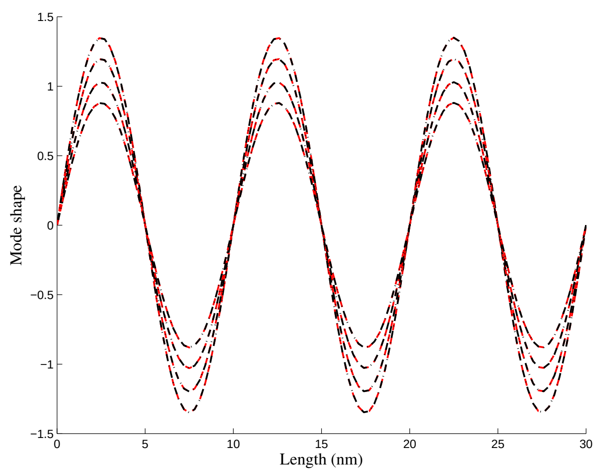

(c) Mode 6

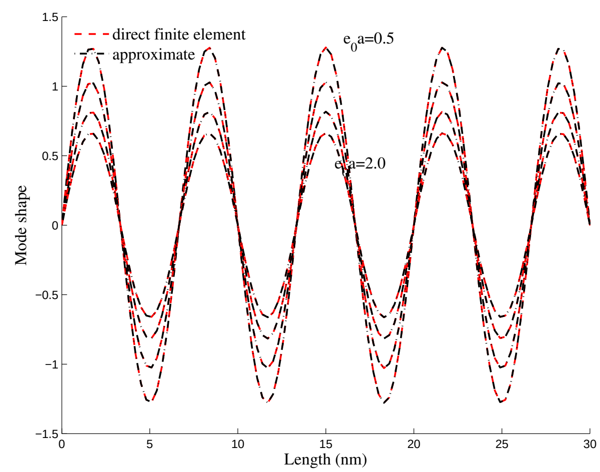

(d) Mode 9

Figure 8.10 – Four selected mode shapes for the bending vibration of DWCNT. Exact finite element results are compared with the approximate analysis based on local eigensolutions. In each subplot four different values of e_0a, namely 0.5, 1.0, 1.5 and 2.0nm have been used (see subplot d).

First 15 nonlocal natural frequencies are shown for four distinct values of e_0a, namely 0.5, 1.0, 1.5 and 2.0nm. In the same figure, natural frequencies obtained using the direct finite element method and the results obtained using the approximate expression (8.44) are also shown. It can be observed that the values obtains using three different approaches are very close. Natural frequencies corresponding to the underlying local system is shown in Figure 8.13. Local frequencies diverge significantly from the nonlocal frequencies for higher frequency indices. The approximate expression of the natural frequency given by Eq. (8.44) is able to capture this quantitative difference very well.

In Figure 8.14 mode shapes corresponding to mode 2, 4, 5, and 6 are shown when the nonlocal parameter $e_0a = 2$nm. We have selected the highest value of e_0a as this leads to maximum inaccuracy of the proposed approximate expressions. Results obtained from the direct finite element and the approximate expression given by Eq. (8.48) are shown in these plots. These mode numbers are selected for illustration only. Results obtained from the direct finite element and the approximate expression given by Eq. (8.48) are shown in these plots. The mode shapes obtain by both approach agree to each other well.

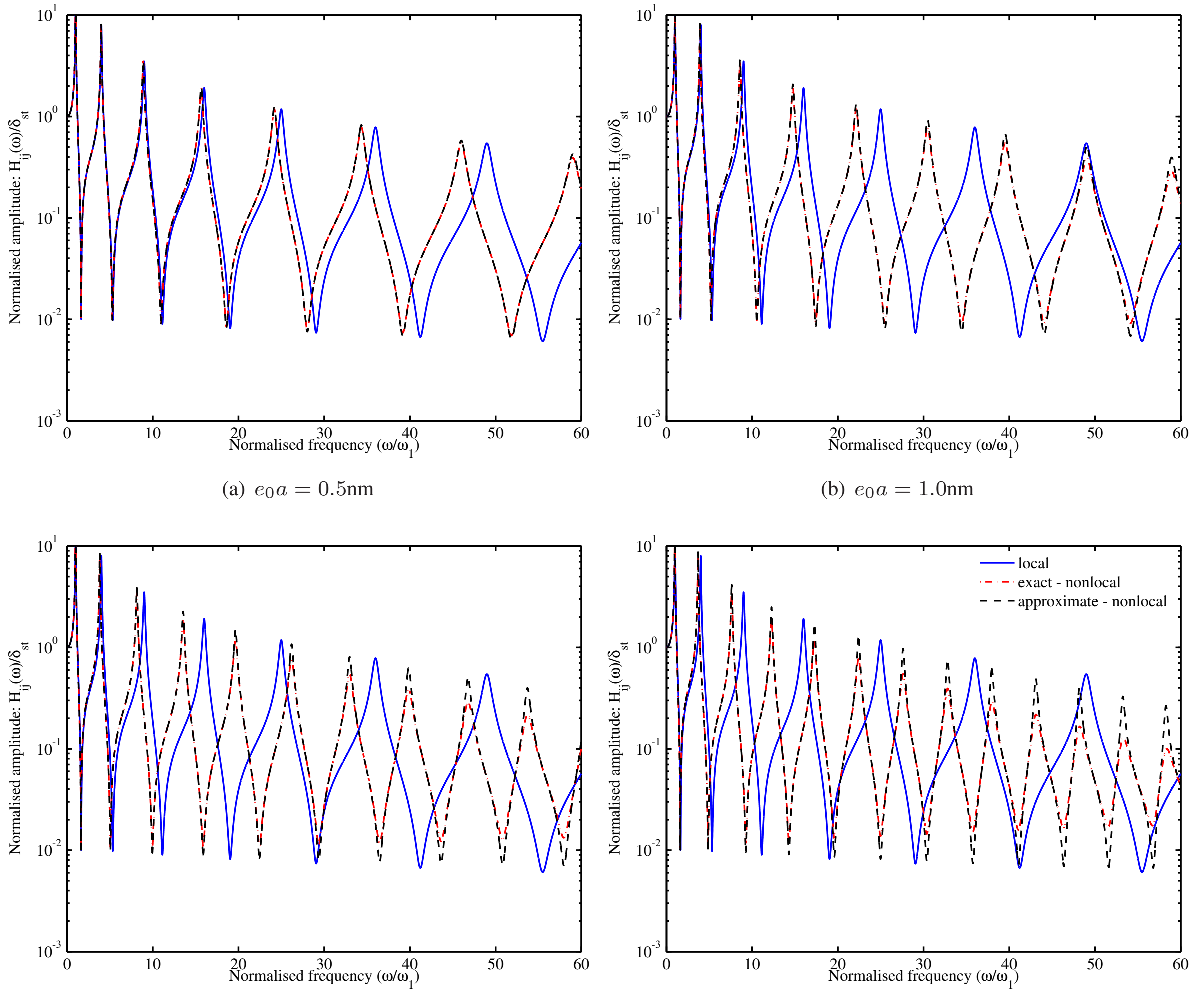

(a) $e_0a = 0.5$nm

(b) $e_0a = 1.0$nm

(c) $e_0a = 1.5$nm

(d) $e_0a = 2.0$nm

Figure 8.11 – Amplitude of the normalised frequency response of the DWCNT $H_{ij}(\omega)$ for $i = 6, j = 8$ for different values of e_0a. Exact finite element results are compared with the approximate analysis based on local eigensolutions.

Finally in Figure 8.15 the amplitude of the frequency response function $H_{ij}(\omega)$ for $i = 475, j = 342$ is shown for the four representative values of the nonlocal parameter. In the x-axis, excitation frequency normalised with respect to the first local frequency is considered. The frequency response is normalise by the static response d_{st} (that is the response when the excitation frequency is zero rad/s). The frequency response function of the underlying local model is also plotted to show the difference between the local and nonlocal response. For the nonlocal system, the frequency response is obtained by the direct finite element method and the approximation derived in section 8.4. As proportional damping model is assumed, the off-diagonal part of the modal damping matrix is a null matrix. For this case the approximate solution match the exactly to the results obtained from the direct finite element method. The dynamic response of the nonlocal system becomes very different from the corresponding local system for higher frequency values and higher values of the nonlocal parameter e_0a. The proposed approximate expression of the transfer function given in Eq. (8.59) can be used to understand this significant different behaviour.

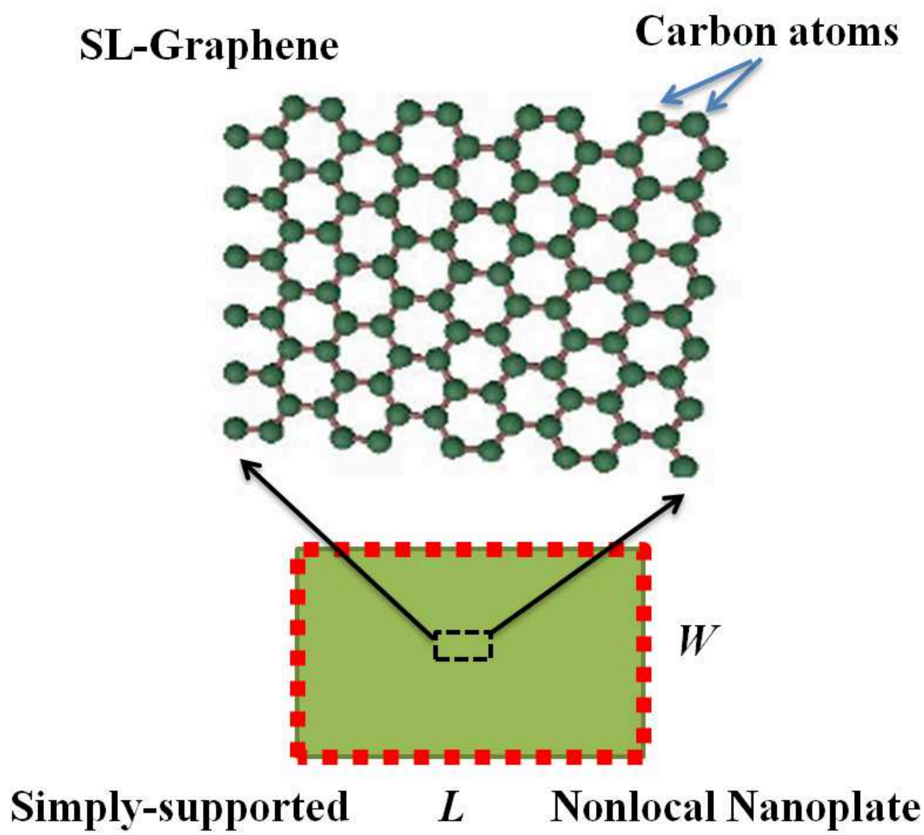

Figure 8.12 – Transverse vibration of a rectangular (L=20nm, W=15nm) single-layer graphene sheet (SLGS) with simply supported boundary condition along the four edges.

8.6. Summary

Nonlocal elasticity is a promising theory for the modelling of nanoscale dynamical systems such as carbon nantotubes and graphene sheets. A finite element approach is proposed for dynamic analysis of general nonlocal structures. Explicit closed-form expressions of element mass and stiffness matrices of nanorods, nanobeams and nanoplates have been derived. The mass matrix can be decomposed into two parts, namely the classical local mass matrix $\mathbf{M}_0$ and a nonlocal part denoted by $\mathbf{M}_\mu$. The nonlocal part of the mass matrix is scale-dependent and vanishes for systems with large length-scale. New analytical approaches have been developed to understand the dynamic behaviour of general discrete nonlocal systems. Approximate expressions for nonlocal natural frequencies, mode shapes and frequency response functions have been derived. Major theoretical contributions made in this paper include the following results:

– An undamped nonlocal system will have classical normal modes provided the nonlocal part of the mass matrix satisfy the condition $\mathbf{K}\mathbf{M}_0^{-1}\mathbf{M}_\mu = \mathbf{M}_\mu\mathbf{M}_0^{-1}\mathbf{K}$ where $\mathbf{K}$ is the stiffness matrix.

– A viscously damped nonlocal system with damping matrix $\mathbf{C}$ will have classical normal modes provided $\mathbf{C}\mathbf{M}_0^{-1}\mathbf{K} = \mathbf{K}\mathbf{M}_0^{-1}\mathbf{C}$ and $\mathbf{C}\mathbf{M}_0^{-1}\mathbf{M}_\mu = \mathbf{M}_\mu\mathbf{M}_0^{-1}\mathbf{C}$ in addition to the previous condition.

– Natural frequency of a general nonlocal system can be expressed as $\lambda_j \approx \frac{\omega_j}{\sqrt{1+M'_{\mu_{jj}}}}, \forall j = 1, 2, \cdots$ where ω_j are the corresponding local frequencies and $M'_{\mu_{jj}}$ are the elements of nonlocal part of the mass matrix in the modal coordinate.

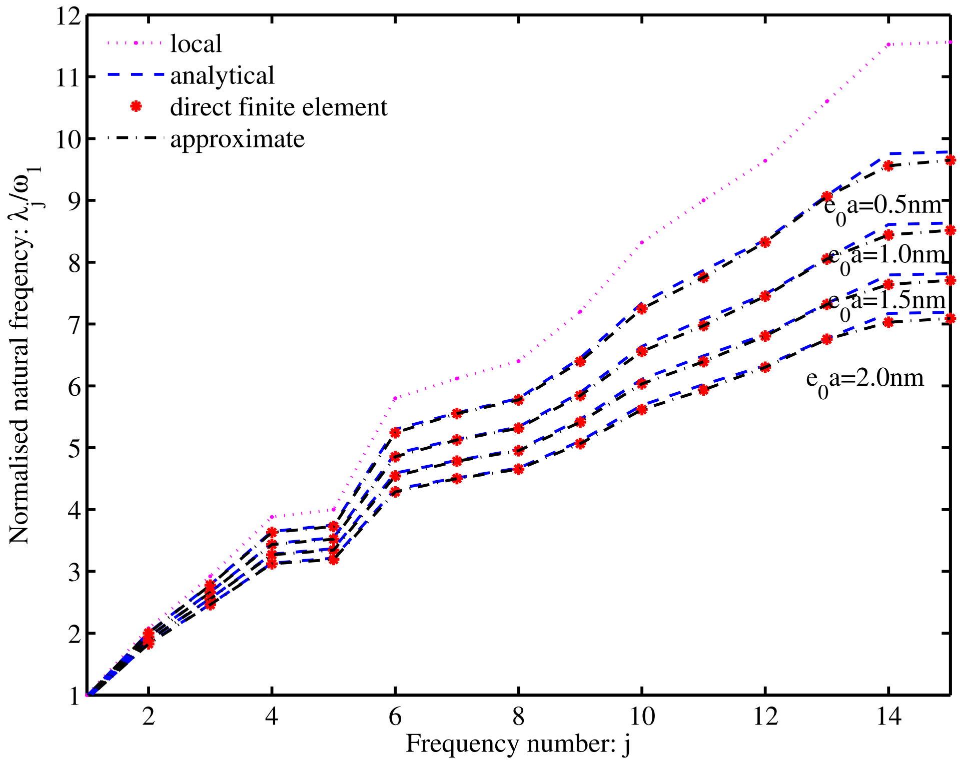

Figure 8.13 – The variation of first 15 undamped natural frequencies for the transverse vibration of SLGS. Four representative values of e_0a (in nm) are considered.

– Every nonlocal normal mode can be expressed as a sum of two principal components as $\mathbf{u}_j \approx \mathbf{x}_j + (\sum_{k\neq j}^{n} \frac{\lambda_j^2}{(\lambda_k^2-\lambda_j^2)} \frac{M'_{\mu_{kj}}}{(1+M'_{\mu_{kk}})}\mathbf{x}_k), \forall j = 1, 2, \cdots$. One of them is parallel to the corresponding local mode $\mathbf{x}_j$ and the other is orthogonal to it.

The theoretical results obtained in the paper are applied to three representative problems, namely (a) axial vibration of a single-walled carbon nanotube, (b) bending vibration of a double-walled carbon nanotube, and (c) transverse vibration of a single-layer graphene sheet. These three systems are modelled by nonlocal rod, beam and plate respectively. Among these three systems, only the nonlocal rod model satisfy the condition of existence of classical normal modes. For the other two systems it was observed that the proposed approximate expressions of nonlocal natural frequencies, mode shapes and frequency response functions provide acceptable accuracy. The results obtained in the paper give physical insights into the dynamic behaviour of discrete nonlocal systems which can be understood in the light of well known dynamic behaviour of the underlying local systems.

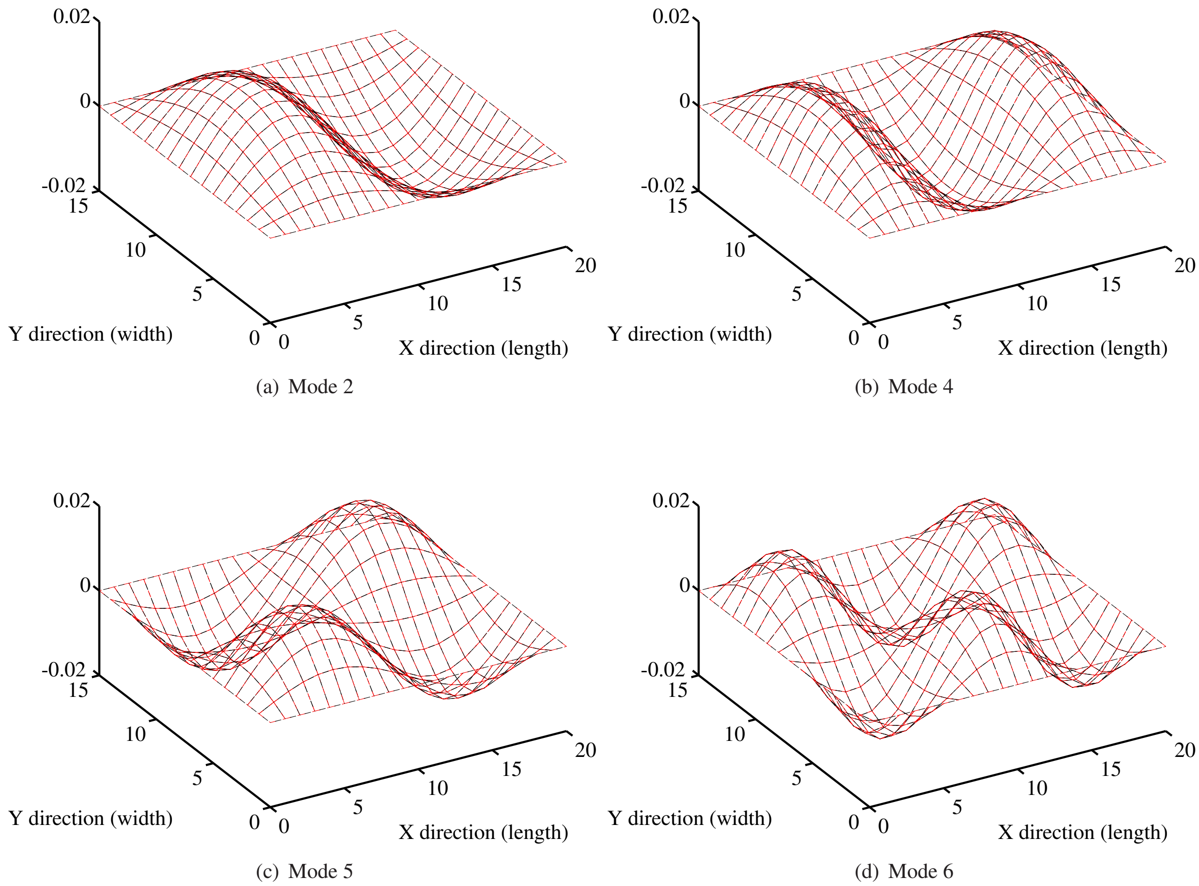

(a) Mode 2

(b) Mode 4

(c) Mode 5

(d) Mode 6

Figure 8.14 – Four selected mode shapes for the transverse vibration of SLGS for $e_0a = 2$nm. Exact finite element results (solid line)are compared with the approximate analysis based on local eigensolutions (dashed line).

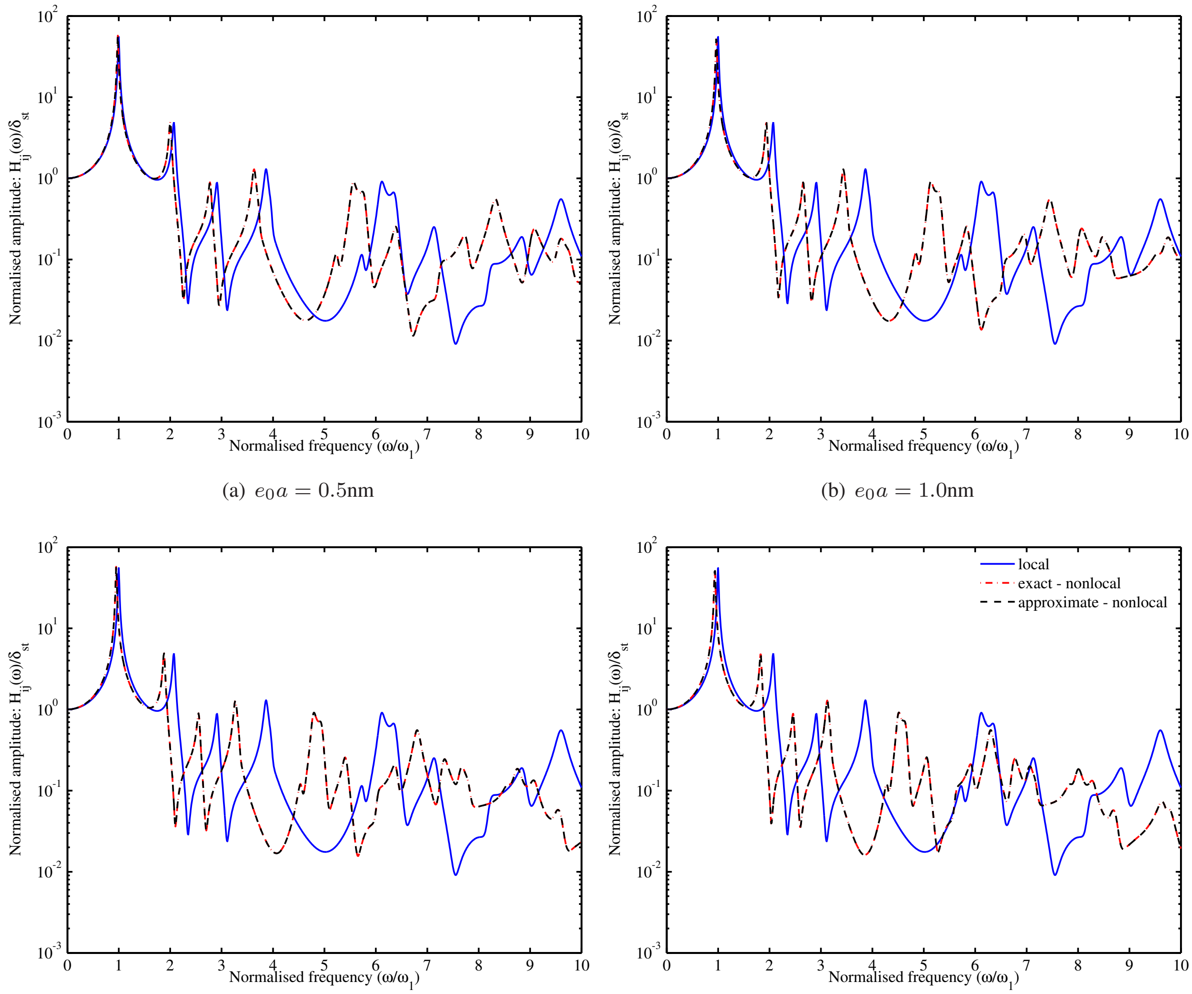

(a) $e_0a = 0.5$nm

(b) $e_0a = 1.0$nm

(c) $e_0a = 1.5$nm

(d) $e_0a = 2.0$nm

Figure 8.15 – Amplitude of the normalised frequency response $H_{ij}(\omega)$ for $i = 475, j = 342$ of the SLGS for different values of e_0a. Exact finite element results are compared with the approximate analysis based on local eigensolutions.

Chapter 9

Bibliography

[ADH 06] ADHIKARI S., "Damping modelling using generalized proportional damping", *Journal of Sound and Vibration*, vol. 293, num. 1-2, p. 156-170, May 2006.

[ADH 13] ADHIKARI S., MURMU T., MCCARTHY M., "Dynamic finite element analysis of axially vibrating nonlocal rods", *Finite Elements in Analysis and Design*, vol. 63, num. 1, p. 42-50, 2013.

[AKG 11] AKGOZ B., CIVALEK O., "Strain gradient elasticity and modified couple stress models for buckling analysis of axially loaded micro-scaled beams", *International Journal of Engineering Science*, vol. 49, num. 11, p. 1268-1280, 2011.

[AKG 12] AKGOZ B., CIVALEK O., "Free vibration analysis for single-layered graphene sheets in an elastic matrix via modified couple stress theory", *Materials & Design*, vol. 42, num. 164, 2012.

[AKS 11] AKSENCER T., AYDOGDU M., "Levy type solution method for vibration and buckling of nanoplates using nonlocal elasticity theory", *Physica E-Low-Dimensional Systems & Nanostructures*, vol. 43, num. 954, 2011.

[ANS 10] ANSARI R., RAJABIEHFARD R., ARASH B., "Nonlocal finite element model for vibrations of embedded multi-layered graphene sheets", *Computational Materials Science*, vol. 49, num. 831, 2010.

[ANS 11] ANSARI R., ARASH B., ROUHI H., "Vibration characteristics of embedded multi-layered graphene sheets with different boundary conditions via nonlocal elasticity", *Composite Structures*, vol. 93, num. 2419, 2011.

[ARA 12] ARASH B., WANG Q., "A review on the application of nonlocal elastic models in modeling of carbon nanotubes and graphenes", *Computational Materials Science*, vol. 51, num. 303, 2012.

[ART 11] ARTAN R., TEPE A., "Nonlocal Effects in Curved Single-Walled Carbon Nanotubes", *Mechanics of Advanced Materials and Structures*, vol. 18, num. 347, 2011.

[AYD 09] AYDOGDU M., "Axial vibration of the nanorods with the nonlocal continuum rod model", *Physica E*, vol. 41, num. 5, p. 861-864, 2009.

[AYD 11] AYDOGDU M., FILIZ S., "Modeling carbon nanotube-based mass sensors using axial vibration and nonlocal elasticity", *Physica E-Low-Dimensional Systems & Nanostructures*, vol. 43, num. 1229, 2011.

[AYD 12] AYDOGDU M., "Axial vibration analysis of nanorods (carbon nanotubes) embedded in an elastic medium using nonlocal elasticity", *Mechanics Research Communications*, vol. 43, num. 34, 2012.

[BAB 11] BABAEI H., SHAHIDI A., "Small-scale effects on the buckling of quadrilateral nanoplates based on nonlocal elasticity theory using the Galerkin method", *Archive of Applied Mechanics*, vol. 81, num. 1051, 2011.

[BRO 07] BRODKA A., KOLOCZEK J., BURIAN A., "Application of molecular dynamics simulations for structural studies of carbon nanotubes", *Journal of Nanoscience and Nanotechnology*, p. 7-1505, 2007.

[CAU 65] CAUGHEY T. K., O'KELLY M. E. J., "Classical normal modes in damped linear dynamic systems", *Transactions of ASME, Journal of Applied Mechanics*, vol. 32, p. 583-588, September 1965.

[CHA 12] CHANG T., "Finite Element Analysis on Vibration of Nanorods with Heterogeneous Property and Non-Uniform Cross Section", *Advanced Science Letters*, vol. 13, num. 360, 2012.

[CHO 10] CHOWDHURY R., ADHIKARI S., WANG C. Y., SCARPA F., "A molecular mechanics approach for the vibration of single walled carbon nanotubes", *Computational Materials Science*, vol. 48, num. 4, p. 730-735, 2010.

[CHO 11a] CHOWDHURY R., ADHIKARI S., SCARPA F., "Vibrational analysis of ZnO nanotubes: A molecular mechanics approach", *Applied Physics A*, vol. 102, num. 2, p. 301-308, 2011.

[CHO 11b] CHOWDHURY R., ADHIKARI S., SCARPA F., FRISWELL M. I., "Transverse vibration of single layer graphene sheets", *Journal of Physics D: Applied Physics*, vol. 44, num. 20, p. 205401:1-11, 2011.

[DAW 84] DAWE D., *Matrix and Finite Element Displacement Analysis of Structures*, Oxford University Press, Oxford, UK, 1984.

[ERI 83] ERINGEN A. C., "On Differential-Equations of Nonlocal Elasticity and Solutions of Screw Dislocation and Surface Waves", *Journal of Applied Physics*, vol. 54, num. 9, p. 4703-4710, 1983.

[GÉR 97] GÉRADIN M., RIXEN D., *Mechanical Vibrations*, John Wiely & Sons, New York, NY, second edition, 1997, Translation of: Théorie des Vibrations.

[HEI 10] HEIRECHE H., TOUNSI A., BENHASSAINI H., BENZAIR A., BENDAHMANE M., MISSOURI M., MOKADEM S., "Nonlocal elasticity effect on vibration characteristics of protein microtubules", *Physica E-Low-Dimensional Systems & Nanostructures*, vol. 42, num. 2375, 2010.

[IIJ 93] IIJIMA S., ICHIHASHI T., "Single-shell carbon nanotubes of 1-nm diameter", *Nature*, p. 363-603, 1993.

[JOM 11] JOMEHZADEH E., NOORI H., SAIDI A., "The size-dependent vibration analysis of micro-plates based on a modified couple stress theory", *Physica E-Low-Dimensional Systems & Nanostructures*, vol. 43, num. 877, 2011.

[KAH 10] KAHROBAIYAN M. H., ASGHARI M., RAHAEIFARD M., AHMADIAN M., "Investigation of the size-dependent dynamic characteristics of atomic force microscope microcantilevers based on the modified couple stress theory", *International Journal of Engineering Science*, vol. 48, num. 12, p. 1985-1994, 2010.

[KAR 10] KARAOGLU P., AYDOGDU M., "On the forced vibration of carbon nanotubes via a non-local Euler-Bernoulli beam model", *Proceedings of the Institution of Mechanical Engineers Part C-Journal of Mechanical Engineering Sience*, vol. 224, num. C2, p. 497-503, 2010.

[KIA 98] KIANG C., ENDO M., AJAYAN P., DRESSELHAUS G., DRESSELHAUS M., "Size effects in carbon nanotubes", *Physical Review Letters*, vol. 81, num. 1869, 1998.

[KIA 11] KIANI K., "Small-scale effect on the vibration of thin nanoplates subjected to a moving nanoparticle via nonlocal continuum theory", *Journal of Sound and Vibrations*, vol. 330, num. 20, p. 4896-4914, 2011.

[MEI 97] MEIROVITCH L., *Principles and Techniques of Vibrations*, Prentice-Hall International, Inc., New Jersey, 1997.

[MUR 09] MURMU T., PRADHAN S. C., "Vibration analysis of nano-single-layered graphene sheets embedded in elastic medium based on nonlocal elasticity theory", *Journal of Applied Physics*, vol. 105, num. 1, 2009.

[MUR 10] MURMU T., ADHIKARI S., "Nonlocal effects in the longitudinal vibration of double-nanorod systems", *Physica E: Low-dimensional Systems and Nanostructures*, vol. 43, num. 1, p. 415-422, 2010.

[MUR 11a] MURMU T., ADHIKARI S., "Nonlocal vibration of bonded double-nanoplate-systems", *Composites Part B: Engineering*, vol. 42, num. 7, p. 1901-1911, 2011.

[MUR 11b] MURMU T., ADHIKARI S., "Nonlocal vibration of carbon nanotubes with attached buckyballs at tip", *Mechanics Research Communications*, vol. 38, num. 1, p. 62-67, 2011.

[MUR 12a] MURMU T., ADHIKARI S., "Nonlocal elasticity based vibration of initially pre-stressed coupled nanobeam systems", *European Journal of Mechanics - A/Solids*, vol. 34, num. 1, p. 52-62, 2012.

[MUR 12b] MURMU T., ADHIKARI S., MCCARTHY M., "Vibration response of double-walled carbon nanotubes subjected to an externally applied longitudinal magnetic field: A nonlocal elasticity approach", *Journal of Sound and Vibration*, vol. 331, num. 23, p. 5069-5086, 2012.

[NAR 11a] NARENDAR S., GOPALAKRISHNAN S., "Axial wave propagation in coupled nanorod system with nonlocal small scale effects", *Composites Part B-Engineering*, vol. 42, num. 2013, 2011.

[NAR 11b] NARENDAR S., GOPALAKRISHNAN S., "Spectral Finite Element Formulation for Nanorods via Nonlocal Continuum Mechanics", *Journal of Applied Mechanics-Transactions of the Asme*, vol. 78, 2011.

[PAC 08] PACILE D., MEYER J., GIRIT C., ZETTL A., "The two-dimensional phase of boron nitride: Few-atomic-layer sheets and suspended membranes", *Applied Physics Letters*, Page 92, 2008.

[PED 03] PEDDIESON J., BUCHANAN G., MCNITT R., "Application of nonlocal continuum models to nanotechnology", *International Journal of Engineering Science*, vol. 41, num. 305, 2003.

[PET 98] PETYT M., *Introduction to Finite Element Vibration Analysis*, Cambridge University Press, Cambridge, UK, 1998.

[PHA 10] PHADIKAR J. K., PRADHAN S. C., "Variational formulation and finite element analysis for nonlocal elastic nanobeams and nanoplates", *Computational Materials Science*, vol. 49, num. 3, p. 492-499, 2010.

[PIS 09] PISANO A. A., SOFI A., FUSCHI P., "Nonlocal integral elasticity: 2D finite element based solutions", *International Journal of Solids and Structures*, vol. 46, num. 21, p. 3836-3849, 2009.

[PRA 12] PRADHAN S., "Nonlocal finite element analysis and small scale effects of CNTs with Timoshenko beam theory", *Finite Elements in Analysis and Design*, vol. 50, num. 8, 2012.

[RAY 77] RAYLEIGH L., *Theory of Sound (two volumes)*, Dover Publications, New York, 1945 re-issue, second edition, 1877.

[TAN 08] TANG C., MENG L., SUN L., ZHANG K., ZHONG J., "Molecular dynamics study of ripples in graphene nanoribbons on 6H-SiC(0001): Temperature and size effects", *Journal of Applied Physics*, vol. 104, num. 1, 2008.

[WAN 08] WANG C. M., DUAN W. H., "Free vibration of nanorings/arches based on nonlocal elasticity", *Journal of Applied Physics*, vol. 104, num. 1, 2008.

[WAR 09] WARNER J., SCHAFFEL F., RUMMELI M., BUCHNER B., "Examining the Edges of Multi-Layer Graphene Sheets", *Chemistry of Materials*, p. 21-2418, 2009.

[WON 97] WONG E., SHEEHAN P., LIEBER C., "Nanobeam mechanics: Elasticity, strength, and toughness of nanorods and nanotubes", *Science*, p. 277-1971, 1997.

[YAN 08] YANG J., JIA X., KITIPORNCHAI S., "Pull-in instability of nano-switches using nonlocal elasticity theory", *Journal of Physics D-Applied Physics*, vol. 41, num. 1, 2008.

[ZIE 91] ZIENKIEWICZ O. C., TAYLOR R. L., *The Finite Element Method*, McGraw-Hill, London, fourth edition, 1991.